Thank you very much to the editor for facilitating the review process and to both referees for providing construction feedback on the submitted manuscript. The suggestions and corrections have been incorporated in the revised manuscript and are tracked in blue.

Author Comments to Anonymous Referee #1

We thank the referee for the very thoughtful and valuable comments which we have addressed below.

Comment by Referee 1) The conclusion of dimer formation being important relies on the kinetic modelling with dimers included in the model. This requires an assumption of initial particle composition which in this work is approximated by first calculating the particle composition based on partitioning theory and previously measured VBS and then calculating the monomer/dimer equilibrium (p. 10006, l. 16-21). However, if the SOA contains dimers, these compounds would be accounted for in the lower volatility bins when VBS was determined from the growth experiments, not by the VBS bins corresponding to the SVOC monomers. The authors estimate the dimer formation time scale to be only a fraction of a second (p. 10014, l. 4-5) which would suggest that the dimers would have been formed also in the growth experiments where VBS was determined and would therefore contribute to the lowest VBS bins. As most of the particle mass is estimated to consist of dimers (p. 10013, l. 8) the way the dimers are treated in the calculation of initial composition could make a large difference on results. Could the authors comment on how big error this could cause on their results and what would be the possible consequences of this regarding their conclusions?

Reply: *The reviewer is correct in that the initial assumption of particle composition is based on a traditional VBS distribution. Although the VBS parameters are influenced to some small amount by dimer formation during the SOA formation process, it has been shown by Cappa and Wilson (2011) that fits to such growth experiments are not particularly sensitive to condensed-phase reactions through the application of their modified VBS model, termed in that paper the sequential equilibrium partitioning model. This is because traditional SOA growth experiments are most sensitive to production of new material from the continuing gas-phase reaction, which is unaffected by reactions in the condensed phase. In other words, it is not correct that dimer/oligomer formation necessarily shows up as an increase in yield in the lower volatility bins of the VBS at the expense of higher volatility bins, and the point is that simple parameterizations based on growth experiments do not provide clear information on the contribution of dimerization, etc..*

The reviewer also makes the observation that the way dimers are treated in the calculation of the initial composition could make a large difference in the results. We have considered the potential influence of the lower volatility bins from the VBS distribution being dimers. As we do not know which VBS bins the reviewer suspects are particularly reflective of dimers, we will make an assumption that those with C = 0.01 and 0.1 ug/m3 are "dimers" and those with higher C* values are monomers. (Note: C* = 0.01 ug/m3 is the lowest bin considered in the VBS parameterization we have used). In this case, a relatively small amount of the total mass would be in the form of dimers to begin with, but would not have zero vapor pressure (as we assumed in our case study). These species would thus be subject to direct evaporation as well as thermal decomposition. As the C* values are relatively "high" from the perspective of evaporation in a*

TD, these species would tend to contribute to evaporation at lower temperatures. This would in turn lead to an adjustment in the kf, kr and Ea values that would be needed to fit the observations, most likely with a somewhat lower Ea to slow down evaporation from the "non-volatile" dimers at these same temperatures. An additional consideration is the amount of mass that is found in what might be considered "dimer" bins. In the figure below, we show the distribution of particulate mass at 500 ug/m3 total OA mass for the VBS distribution we have used (Pathak et al., 2007). The amount of mass that is in these bins is very small, and thus they would not have a controlling effect on the evaporation behavior in the simulations. Thus, even if these bins were reflective of the influence of dimers, they would not strongly affect our measurements.

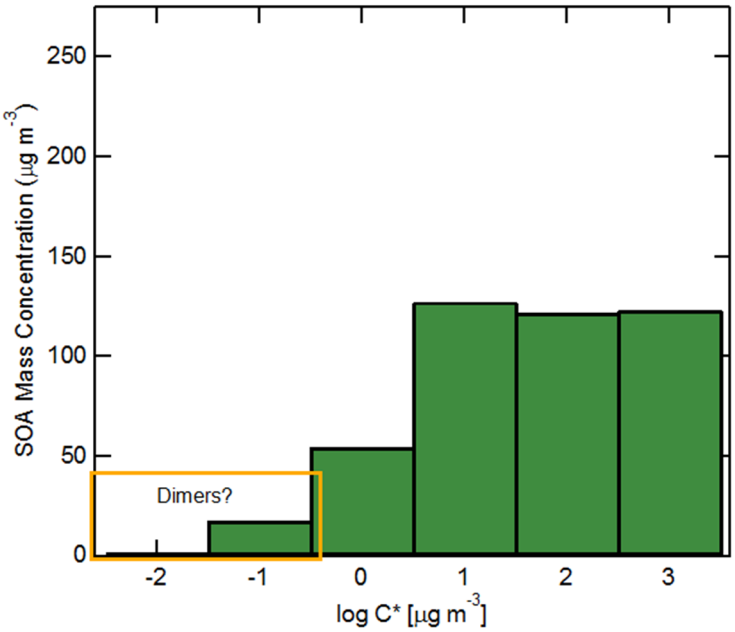

Comment by Referee 2) It is said that the dimers were assumed non-volatile. Were all the VBS bins treated the same way regarding dimer formation? Is it justified to assume that the dimers formed from the compounds in the most volatile VBS bin would also be non-volatile? How would it change the results if the dimers formed from the most volatile SVOCs would evaporate (even though much slower than the monomers)?

Reply: *Yes, all of the VBS bins were treated the same way regarding dimer formation i.e. they all had the same kf, kr and ΔEa. The reviewer raises a good point that the dimers formed from the most volatile SVOCs might evaporate directly more readily than dimers formed from less volatile monomers. The assumption built into the dimer decomposition model is that each bin of dimers will thermally decompose before they would evaporate directly. This thus represents a limiting case. However, we have also presented an alternative model (the low-volatility compound model), in which the volatilities of the compounds comprising the SOA are determined by data fitting and it is assumed that all of these compounds can directly evaporate. This is in effect a second limiting case. The model scenario suggested by the reviewer is a combination of the two models. It is reasonable to think that reality exists somewhere in between these two limiting*

cases, and is something which we will certainly be exploring in future work. However, to the reviewers more specific question of how it would influence the results, the answer is that it would depend on exactly how the vapor pressures of the dimers were specified as we do not know this a priori. Direct evaporation of dimers would compete with decomposition+evaporation, and lead to different fit parameters. Most likely, the decomposition rate at a given temperature would end up decreasing because of the increase in net evaporation from direct dimer evaporation. This would translate to a decrease in ΔEa or an adjustment in the kf/kr values.

Comment by Referee 3) p. 10004, eq. 2: The VFR was calculated based on volume-weighted average diameters. However, based on Fig. 1 the size distributions were rather wide. Did the model consider polydisperse particle population or did it assume monodisperse population? How large uncertainty does the use of average diameter for VFR cause in respect the comparison of measurement and model?

Reply: *The reviewer is correct in pointing out that by treating the model SOA as monodisperse while the experimental SOA is polydisperse is not a perfect comparison. However, over the range of Dp = 30 to 400 nm the maximum difference between the two predicted curves for the dimer decomposition model is VFR = 0.07 (See accompanying figure). Although all of the model predictions using the same kr, kf, Keqm and deltaEa while varying the particle diameter agree reasonably well with the experimental observations and with each other, a unique set of fit parameters could equally be determined for the different sized particles. The maximum difference between particles of different varying diameter for the low volatility scenario is also small (VFR = 0.11) and the low-volatility product distribution could be further adjusted to provide better model/observation agreement for each particle size. Regardless, the common feature amongst all of the thermodenuder model scenarios is that the particle evaporation can be explained assuming that the particles are either composed of a large fraction of dimers that thermally decompose or of low-volatility compounds that evaporate directly (or some combination thereof).*

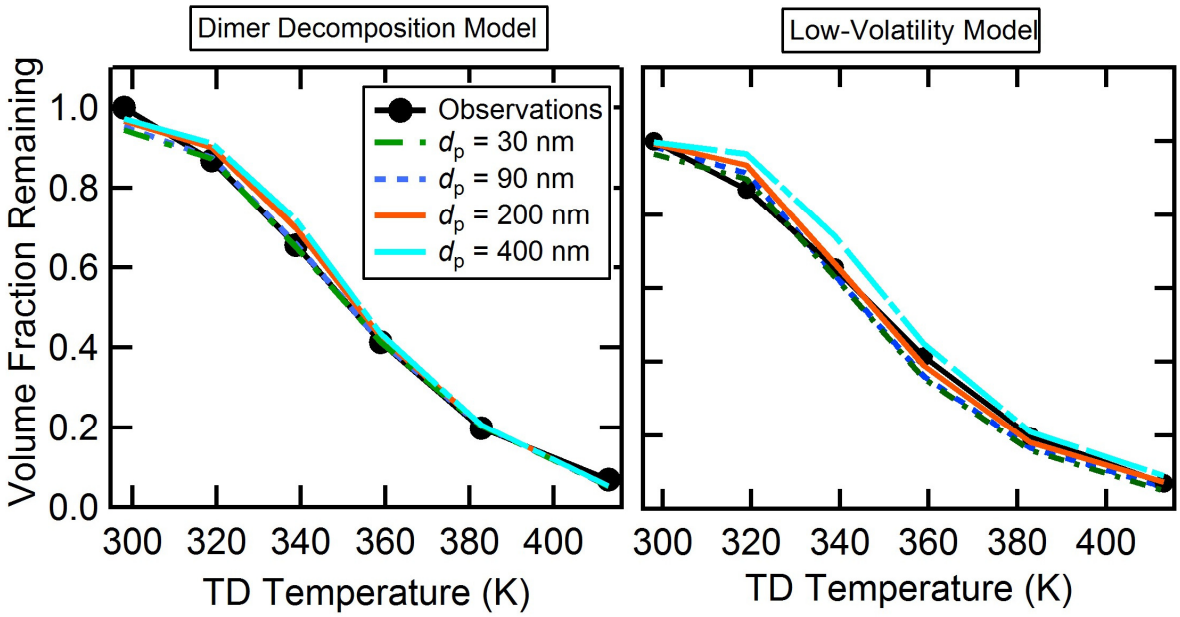

Comment by Referee 4) p. 10010, l. 2-6: Evaporation upon isothermal dilution can be rapid for the most volatile SVOCs. Therefore, the composition of diluted SOA can be different, especially if large fraction of initial mass was of the most volatile SVOCs.

Reply: *The reviewer points out that when OA is composed of a large fraction of SVOCs then there will be rapid evaporation of these compounds upon isothermal dilution which will likely lead to changes in particle composition. However, for α-pinene+O_3 SOA, this and other studies have measured both directly and indirectly that rapid dilution does not induce instantaneous evaporation; instead, it takes minutes for the particles to respond to any significant extent. We note that this behavior for SOA is very different than it is for particles made of lubricating oil. Lubricating oil particles exhibit near instantaneous evaporation in response to dilution or vapor stripping. Given that we observe no mass loss upon rapid dilution, the composition of the SOA formed at high C_{OA} should not change upon rapid dilution as it would for a semi-volatile aerosol such as lubricating oil.*

Comment by Referee 5) The assumption of initial composition of particles determines to a large extend the modeled mass thermograms. In the low-volatility version of the model the total concentration of each compound C_i,tot was calculated with the exponential equation (p. 10018, l. 11). Could the authors clarify the use of this equation a bit? It is not clear why such exponential equation is used and if it is physically justified. Did the a1, a2, a3 and a4 have same values for each C*? It is said (p. 10018, l. 12-16) that the a values were determined for one certain C_OA value, however later the same set of a values is used for varying C_OA values. Is this consistent use of the a values and the equation for C_i,tot.

Reply: *The functional form used here is entirely empirical, based of that used in (Cappa and Jimenez, 2010). To quote them: "This form was chosen in part because it is generally consistent with observations of the volatility distributions determined for laboratory secondary OA (Presto and Donahue, 2006)and for OA from diesel and woodsmoke emissions (Robinson et al., 2007), but more importantly because it was found to provide generally good agreement between the model and observations." Regarding the question "Did the a1, a2, a3 and a4 have same values for each C*" we wish to clarify that the parameters determine the distribution of mass with respect to C* through the relationship given in the text: ($C_{i,tot}$ = a1+a2*exp(a3*(logC*)+a4)). In other words, C* does not depend on the 'a' values. It is the $C_{i,OA}$ values that depend on the a values (and C*). . To the question regarding the use of the same values for multiple C_{OA}'s, we should clarify that the shape of the $C_{i,tot}$ curve was determined using the same set of parameters at each C_{OA} (with those parameters determined from fitting the observations for one particular C_{OA}, as discussed in the manuscript). However, the absolute values of $C_{i,tot}$ were scaled using a constant multiplicative factor for each C_{OA} such that the absolute model C_{OA} matched the observed C_{OA} to which it was compared. Given the functional form used ($C_{i,tot}$ = a1+a2*exp(a3*(logC*)+a4)), this amounts to scaling the parameters and a1 and a2 by a C_OA specific constant. In other words, $C_{i,tot}(C_{OA})$ = b*$C_{i,tot}$(reference case) = b*(a1+a2*exp(a3*logC*)+a4))) where b is set for each C_{OA} value but is independent of C*. This will be clarified in the revised manuscript, although it should be noted that it has no material impact on the observations given that the functional form is somewhat (although not entirely) arbitrary in the first place.*

Technical comments:
p. 10009, l. 23: There should probably be ‘high’ before ‘C_OA’.
This has been fixed.

Figure 1: I find the x-axis numbers confusing as one would by quickly looking think that the average diameter was 2-4 nm, instead of 20-40 nm. I would thus recommend modifying the x-axis.

The figure has been updated.

Interactive comment on Atmos. Chem. Phys. Discuss., 15, 9997, 2015.
C2315

References

Cappa, C. D., and Jimenez, J. L.: Quantitative estimates of the volatility of ambient organic aerosol, Atmospheric Chemistry and Physics, 10, 5409-5424, 10.5194/acp-10-5409-2010, 2010.
Pathak, R. K., Presto, A. A., Lane, T. E., Stanier, C. O., Donahue, N. M., and Pandis, S. N.: Ozonolysis of alpha-pinene: parameterization of secondary organic aerosol mass fraction, Atmospheric Chemistry and Physics, 7, 3811-3821, 2007.
Presto, A. A., and Donahue, N. M.: Investigation of alpha-pinene plus ozone secondary organic aerosol formation at low total aerosol mass, Environmental Science & Technology, 40, 3536-3543, 10.1021/es052203z, 2006.
Robinson, A. L., Donahue, N. M., Shrivastava, M. K., Weitkamp, E. A., Sage, A. M., Grieshop, A. P., Lane, T. E., Pierce, J. R., and Pandis, S. N.: Rethinking organic aerosols: Semivolatile emissions and photochemical aging, Science, 315, 1259-1262, 10.1126/science.1133061, 2007.

Author Comments to Referee Pontus Roldin

We thank the referee very much for providing insightful feedback on our manuscript. Below we have responded to the specific questions and suggestions from the referee.

Many of the referee's comments dealt with the issue that our model assumes well-mixed particles, whereas actual SOA may have (and likely does have) a relatively low viscosity. We have made more explicit the limitations of this assumption on our modeling by adding additional sentences, as well as addressing the specific comments.

Comment by Referee 1)"In addition, several experiments have observed slower than expected room temperature evaporation of both ambient (Vaden et al., 2011) and laboratory generated (Saleh et al., 2013; Grieshop et al., 2007; Wilson et al., 2015) SOA during isothermal dilution." Vaden et al., 2011 also studied laboratory generated SOA. Refer to Vaden et al., 2011 for the laboratory generated SOA too.

We have added a reference to Vaden.

Comment by Referee 2) P 10002, L3: You use the term "*homogeneous nucleation*" to refer to how the SOA particles were generated. I have also used this expression in previous publications when I referred to new particle formation during no-seed SOA particle formation experiments. However, I don't know if this is correct. Lately I have started to use "formation of nano condensation nuclei (nano-CN)" instead, with a reference to McMurry P. H., Kulmala, M., Worsnop D. R.: Special Issue on Aerosol Measurements in the 1 nm Range, Aerosol Sci. Technol. 45, I, 2011.

Reply: *We thank the referee for pointing out that there is other possible nomenclature that may more precisely describe the process by which particles are generated in laboratory experiments. The language has been updated to reflect this more precise definition of particle generation and now reads:*

"SOA was formed at various total C_{OA} from the formation and subsequent growth of nano-condensation nuclei that were formed from products of the ozonolysis of gas-phase α-pinene, in excess (Fig. S1)"

Comment by Referee 3) P 10005 L1-L4: "*Here, to provide for more consistent fitting and since no evaporation at room temperature was observed, the fit curves were forced to go through unity at room temperature."*

Change to: "Here, to provide for more consistent fitting and since no evaporation was observed at room temperature, the fit curves were forced to go through unity at room temperature."

This has been changed.

Comment by Referee 4) Sect. 2.4.1 Thermodenuder model. An assumption that I think should be mentioned is that you assumed that the particles behave as liquid droplets (no mass transport limitations in the particle-phase). This may be justified by the relative high temperature in the TD but is probably not entirely true for room-temperature isothermal evaporation.

Reply: *The following has been added to Section 2.4.1 "It was assumed that there were no mass transport limitations within the particle-phase for all evaporating species, i.e. that the surface composition was always equivalent to the bulk composition."*

Comment by Referee 5) P 10006, L14-21: *"If K_{eqm} is large then all condensed-phase species would be in dimer form and, at equilibrium, all gas-phase material would be drawn into the condensed phase. Here, this situation is avoided through the following simplification to determine the initial particle state at the TD inlet. First, the gas/particle (monomer only) equilibrium distribution is calculated given the specified volatility distribution and C_{OA}. Then the monomer/dimer equilibrium in the condensed phase is calculated, and the gas-phase concentrations are set to zero to avoid large amounts of condensing material at the next time step. Since a charcoal denuder is placed immediately after the flowtube, this simplification is physically accurate."*

It is good that you clearly describe the assumptions that you use for the model setup but I think that it would be more physically reasonable to assume that monomers are not dissolved (absorbing) into the dimer SOA volume fraction if you want to limit the growth during next time step. You would then have to simulate (or iteratively derive) the SOA composition at the TD inlet. To assume that the monomers absorbs into the total C_{OA} would not be correct then. Especially for the low SOA loading experiments, I think that you actually need to explicitly simulate how the non-equilibrium SOA formation and dimer/monomer SOA composition changes in the flow-tube.

Reply: *The reviewer raises an important point regarding the initial conditions assumed in the modeling of the SOA evaporation in the TD. There are two important considerations: the nature and distribution of the monomers within the particle phase, independent of dimerization, and the monomer/dimer distribution. Of course, these are coupled phenomena. However, given that our model assumes that the lowest saturation concentration of condensing monomers is 0.1 micrograms/m^3 and further that the abundance of these are very small, the dimer model is—to a reasonable extent—independent of the exact distribution of monomers with respect to their volatility and much more sensitive to the monomer/dimer distribution. Thus, it is reasonable to think of the different K_{eqm} simulations as the key case studies with the initial volatility distribution of monomers as a secondary concern. Put another way, since the monomers in our model evaporate "fast" given their relatively high volatilities the dimer model(s) are not overly sensitive to the monomer volatility distribution. This is not to imply that the exact monomer distribution at the start does not matter, as it certainly does, only that it is substantially less consequential than the monomer/dimer distribution. We fully agree that comprehensive simulation of both formation and evaporation would be the ideal, as it would allow for demonstration of closure. However, accurate simulation of nucleation is no trivial task and beyond the scope of this work.*

In addition, Cappa and Wilson (2011) developed a model that effectively considers particle formation and growth under the assumption that all of the absorbing mass in the particle is converted to non-absorbing at every time step. This is similar to the suggestion of the reviewer that the formation of dimers (non-absorbing mass) be accounted for during particle growth. The particle composition at any given concentration (see their Figure 6) was reasonably similar to the composition predicted from a standard absorptive partitioning model. This implies that more explicit consideration of particle formation, at least in the manner suggested here, will not influence the general conclusions presented in the current work.

We have added the following sentences that describe the nature of model simplifications regarding formation and the likely influence on the current simulations:

"The above simplification for the initial particle state most likely does not provide a true representation of the actual particle composition, just as the assumption regarding only homodimers (discussed below) is a simplification. However, as we ultimately find that the simulation results are much more sensitive to the initial distribution of particulate mass with respect to monomers and dimers than to the specific distribution of monomers with respect to their volatility, these simplifications will influence the details but not the general conclusions arrived at here."

Comment by Referee 6) It would also be good to simulate the vapor stripping in the charcoal denude and not just assume perfect gas-phase removal. Do you have some experimental results to justify this assumption?

Reply: *First, in case it was not clear, we note that transport of the vapors to the TD walls is explicitly simulated within the model such that there is a gradient in vapor concentration from the walls to the center of the cylindrical denuder tube. It is only in the cylindrical "bin" nearest to the wall that perfect gas-phase removal is assumed. That said, the strongest evidence we have for perfect gas-phase removal at the denuder walls, i.e. to the charcoal, comes from experiments performed using lubricating oil (Cappa and Wilson, 2011). In that work, it was found that a model of lubricating oil evaporation, using a separately determined volatility distribution, gave good agreement with observations. If gas-phase removal of vapors at the denuder walls were not "perfect" then the model would have failed and underestimated the extent of evaporation, especially at room temperature. This implies that vapor losses to the walls a near perfect, as would be expected for uptake onto charcoal. We have modified the text as below:*

"Since a charcoal denuder is placed immediately after the flowtube, this simplification is physically reasonable as we have previously found that vapor stripping in charcoal denuders is efficient (Cappa and Wilson, 2011)."

Comment by Referee 7) P 10007, L3-L4: "*The rate at which dimers decompose is governed by k_r and k_f, both of which are likely to be temperature dependent*"

To me it is not entirely clear if you always assume dimer/monomer equilibrium in the model or if you explicitly simulates the non-equilibrium dimer and monomer composition and how it changes in the TD as a function of temperature and evaporation. You need to explain this more clearly.

Reply: *We do not always assume dimer/monomer equilibrium. Dimer/monomer equilibrium is only assumed at the start of the evaporation simulations, i.e. is an initial condition. Once the particles enter the (model) thermodenuder, the kinetics of dimer formation/decomposition are treated explicitly. Several sentences have been added to clarify that the driving force behind evaporation is the perturbation of the dimer/monomer equilibrium by evaporation of monomers and changing K_{eqm} with increasing temperature.*

"As the semi volatile monomers evaporate the equilibrium state is perturbed and the dimers decompose in response, according to the temperature dependent K_{eqm}, to re-establish dimer/monomer equilibrium. Depending on the timescale of dimer formation and decomposition, the dimers and monomers may not be in equilibrium at every step of the model, yet they are constantly forming and decomposing to move towards equilibrium."

Comment by Referee 8) P 10009, L23-24: "*Regardless, it is apparent that the effective volatility of the SOA at C_{OA} is not higher than at low C_{OA} and that, despite the slights differences, the response to heating*"

Add "high"

"Regardless, it is apparent that the effective volatility of the SOA at high C_{OA} is not higher than at low C_{OA} and that, despite the slights differences, the response to heating"

This has been changed.

Comment by Referee 9) P 10013, L20-24: "At smaller K_{eqm} extensive room temperature evaporation occurred as a result of the increasing initial fraction of semi-volatile monomers, a result that is inconsistent with the observations. However, even for the simulations at larger K_{eqm} some evaporation at room temperature was always predicted."

Yes but this is partly because you assumed liquid SOA particles. If the SOA particles are solid-like at room temperature (as suggested by several studies), the evaporation of monomers would slow down substantially once the particle surface layer has been filled with non-volatile dimers.

Reply: *The reviewer raises an important point in noting that the extent of evaporation at room temperature would decrease further if evaporation of the semi-volatile monomers was inhibited by barriers to mass transfer within the particle. We now note this as a potential reason for the room temperature evaporation, although use the terminology "low viscosity" as opposed to "solid" as it is more precise. We have additionally added language in Section 2.4.1 to clarify the assumption of liquid SOA particles, as discussed above.*

"It was assumed that there were no mass transport limitations within the particle phase for all evaporating species, i.e. that the surface composition was always equivalent to the bulk composition."

and

"The simulated room temperature evaporation at larger K_{eqm} may result from the model assumption of liquid-like particles in that if mixing within the particles were slow such that there were a build up at the particle surface of non-volatile dimers then evaporation of monomers that are buried below the surface would be slowed (Roldin et al., 2014)."

Comment by Referee 10) P10015, L15-18: "The range of k_r independently determined here are somewhat larger than the room-temperature k_r suggested by Trump and Donahue (2014) (=1.1×10^{-4} s^{-1}) and Roldin et al. (2014) (=2.8×10^{-5} s^{-1}), which were based on needing an evaporation timescale of ~1 hr for isothermal evaporation (Grieshop et al., 2007;Vaden et al., 2011). However, their estimates may not have fully accounted for the dynamic nature of the system, and thus underestimated the actual dimer decomposition rates compared to that obtained here."

It is true that we used $k_r = 2.8 \times 10^{-5}$ s^{-1} for the results presented in Fig. 6 in Roldin et al. (2014) but we also tested other values of k_r. Including $k_r = 12$ h^{-1} (0.0033 s^{-1}) for a group of relatively abundant (~20 mass %) and shout-lived dimers, in combination with more long-lived but less abundant (1-2 mass %) dimers with $k_r = 1/30$ h^{-1}. We were then able to accurately simulate the nearly particle size independent evaporation of fresh SOa particles from the

experiments in Vaden et al. (2011) (Fig. 77 and Fig. S9-S10 in Roldin et al. (2014)). For these simulations we considered that the particles had a high viscosity in agreement with Abramson et al. (2013). However, with this setup we substantially overestimated the effect of particle ageing in the Teflon chamber on the observed evaporation rates. This can be an indication that the actual oligomer (dimer) fraction of the short-lived dimers was larger than 20 % (maybe close to 100 % as you suggest). This would have limited the effect that VOC wall losses had on the particle composition (and evaporation behavior) when they were aged in the Teflon chamber by Vaden et al. (2011). For these type of experiments I generally think that it is important to also explicitly simulate the SOA formation phase and not just the evaporation stage of the experiments because if you don't get the model to agree with the observations both for the formation and the evaporation experiments something is not correct in the model.

Reply: *As noted above, we completely agree that comprehensive simulation of formation and evaporation is the ideal. However, simulation of nucleation is non-trivial and beyond the scope of this work. Future efforts will aim to explicitly simulate formation in a dynamic manner. That said, we have changed that last sentence above to be:*

"Ultimately, reconciliation of the different timescales indicated for dimer decomposition between the different studies likely will require more detailed consideration of the exact nature of various dimer types with respect to their decomposition and formation timescales, which may not all be identical as assumed here, and of the influence of particle phase on evaporation." We believe that this succinctly captures the important issues raised by the reviewer.

Comment by Referee 11) P10017, L16-21: "*Simulations using the dimer-decomposition model with different starting particle sizes show some dependence on particle size (d_p = 90, 180 and 360 nm), with larger particles having smaller MFRs at a given time (Figure 7a). However, the overall differences are relatively small and reasonably consistent with the observations given that the observations have typically considered a narrower size range than examined here.*"

I still think that the differences between the different particle sizes in Fig 7a is relatively large and it shows that something is missing in the model in order to explain the nearly size independent evaporation rates reported by e.g. Vaden et al. (2011). As mentioned previously several studies (e.g. Virtanen et al., 2010; Abramson et al., 2013 and Zhou et al., 2013) have shown that SOA particles are not liquid-like but viscous tar or even solid-like. I think it would be appropriate to mention that the mass transfer limited diffusion within the particle-phase will also influence the isothermal evaporation but that this was not considered. What was the RH in the flow tube?

Reply: *We have added a statement that mass transfer limitations within the particle phase have not been accounted for here, but can influence evaporation dynamics (see above). Regarding the question about RH, the RH was not directly measured in the flow tube, but was ~30% for all experiments as "house" air was used and this is the typical value. We have added the following sentence:*

"The relative humidity of the air stream was ~30% for all experiments."

Comment by Referee 12) P10020, L13-16: "*If the particles were primarily semi-volatile monomers for which evaporation were limited by diffusion in the particle phase, then changes in viscosity would lead to substantial increases in the observed evaporation rate (Zaveri et al., 2014)"*

Do you mean:

If the particles were primarily semi-volatile monomers for which evaporation were limited by diffusion in the particle phase, then changes in viscosity would lead to substantial increases in the observed evaporation rate (Zaveri et al., 2014)

This we also showed in Roldin et al. (2014) (Fig 5c)

Yes, and the additional citation was added.

Comment by Referee 13) P100, L19-22: "Thus, it seems that a hybrid model where the particles are composed of a substantial fraction of dimers (or oligomers) and some smaller fraction of low-volatility compounds may ultimately provide a more complete description."

I fully agree.

We thank the reviewer for this confirmation.

I suggest that you add the evaporation curves from Vaden et al. (2011) to Fig. 4b and Fig. 7.

These have been added to the figures.

References

Cappa, C. D., and Wilson, K. R.: Evolution of organic aerosol mass spectra upon heating: implications for OA phase and partitioning behavior, Atmospheric Chemistry and Physics, 11, 1895-1911, 10.5194/acp-11-1895-2011, 2011.

Grieshop, A. P., Donahue, N. M., and Robinson, A. L.: Is the gas-particle partitioning in alpha-pinene secondary organic aerosol reversible?, Geophysical Research Letters, 34, L14810 10.1029/2007gl029987, 2007.

Roldin, P., Eriksson, A. C., Nordin, E. Z., Hermansson, E., Mogensen, D., Rusanen, A., Boy, M., Swietlicki, E., Svenningsson, B., Zelenyuk, A., and Pagels, J.: Modelling non-equilibrium secondary organic aerosol formation and evaporation with the aerosol dynamics, gas- and particle-phase chemistry kinetic multilayer model ADCHAM, Atmospheric Chemistry and Physics, 14, 7953-7993, 10.5194/acp-14-7953-2014, 2014.

Trump, E. R., and Donahue, N. M.: Oligomer formation within secondary organic aerosols: equilibrium and dynamic considerations, Atmospheric Chemistry and Physics, 14, 3691-3701, 10.5194/acp-14-3691-2014, 2014.

Vaden, T. D., Imre, D., Beránek, J., Shrivastava, M., and Zelenyuk, A.: Evaporation kinetics and phase of laboratory and ambient secondary organic aerosol, Proceedings of the National Academy of Sciences of the United States of America, 108, 2190-2195, 10.1073/pnas.1013391108, 2011.

The Influences of Mass Loading and Rapid Dilution of Secondary Organic Aerosol on Particle Volatility

Katheryn R. Kolesar[1], Claudia Chen[1,*], David Johnson[1,%] and Christopher D. Cappa[1]

[1] Department of Civil and Environmental Engineering, University of California, Davis, One Shields Avenue, Davis, California 95616, United States

[*] now at: Sustainable Energy Initiative, Santa Clara University, 500 El Camino Real, Santa Clara, California 95053 United States

[%] now at: Advanced Light Source, Lawrence Berkeley National Laboratory, 1 Cyclotron Rd, Berkeley, California 94720, United States

Correspondence to: C.D. Cappa (cdcappa@ucdavis.edu)

Abstract

The thermally-induced evaporation of secondary organic aerosol (SOA) has been characterized for SOA formed from the dark ozonolysis of α-pinene + O_3 at initial mass concentrations ranging from 1 to 800 μg m^{-3}. Temperature-dependent particle size distributions were measured using a thermodenuder and the resulting mass thermograms were compared between the SOA formed at the various SOA mass concentrations. Negligible differences were observed between the mass thermograms for SOA concentrations < 300 μg m^{-3}. At higher SOA concentrations, the observed mass thermograms indicated the SOA was actually slightly less volatile than the SOA at lower concentrations; this is likely an artifact due to either saturation of the gas-phase or to re-condensation during cooling. The thermograms observed when the SOA was formed at high concentrations (>380 μg m^{-3}) and then rapidly isothermally diluted to low concentrations (1-20 μg m^{-3}) were identical to those for the SOA that was initially formed at low concentrations. The experimental results were compared to a kinetic model that simulates particle evaporation upon heating in a thermodenuder for a given input volatility distribution and particle composition. Three cases were considered: 1) the SOA was composed of semi-volatile monomer species with a volatility distribution based on that derived previously from consideration of SOA growth experiments; 2) the initial SOA was composed almost entirely of non-volatile dimers that decompose upon heating into their semi-volatile monomer units, which can then evaporate; and 3) where a volatility distribution was derived by fitting the model to the observed mass thermograms. It was found that good agreement is obtained between model predictions and the observations when the particle composition is either dominated by compounds of low volatility or by dimers. These same models were used to simulate isothermal evaporation of the SOA and were found to be broadly consistent with literature observations that indicate that SOA evaporation occurs with multiple timescales. The use of the semi-volatile monomer volatility distribution fails to reproduce the observed evaporation. The presence of dimers and larger oligomers in secondary organic aerosol formed from products of the reaction of α-pinene and O_3 has been well-established in laboratory studies. However, the timescale and relative importance of the formation of oligomers or low volatility compounds in the growth and evaporation of SOA has been debated. This study provides further support that low volatility compounds and oligomers are formed in α-pinene + O_3 in high abundances and suggests that their formation occurs rapidly upon particle formation.

1 Introduction

Atmospheric aerosol particles have an important impact on human health (Chen et al., 2013) and climate (IPCC, 2014). Organic aerosol (OA) is a significant portion of atmospheric particulate mass, often contributing 20-90% of the fine particle mass world-wide (Saxena and Hildemann, 1996;Andreae and Crutzen, 1997), a major portion of which is secondary organic aerosol (SOA) (Zhang et al., 2005). One pathway through which SOA is formed is when products from the gas-phase oxidation of volatile organic compounds (VOCs) condense onto pre-existing particles or nucleate to form new particles. VOCs are broadly classified as being either biogenic (BVOCs) or anthropogenic (AVOCs). The source of SOA varies with geographical location, with larger contributions of anthropogenic SOA in and around urban areas (Weber et al., 2007) and larger contributions of biogenic SOA in rural areas (Han et al., 2014).

An important source of biogenic SOA is the reaction of unsaturated gas-phase VOCs with O_3. The most globally abundant BVOC compounds are isoprene (C_5H_8) and monoterpenes ($C_{10}H_{16}$) (Kesselmeier and Staudt, 1999). Around 90 Tg C $yr^{-1}$of monoterpenes are emitted from vegetation sources worldwide (Hallquist et al., 2009) of which α-pinene constitutes nearly half (Guenther et al., 1995;Seinfeld and Pankow, 2003). During the formation of SOA from the ozonolysis of α-pinene the aerosol composition and corresponding physical properties have been shown to change as a function of total organic aerosol mass loading (C_{OA}). For example, Shilling et al. (2009) observe that both the O/C ratio and the effective density of α-pinene SOA decrease as C_{OA} increases, most steeply below ~30 μg m^{-3}. Other studies have shown that the mass yield of a variety of SOA, including α-pinene + O_3 SOA, increases as C_{OA} increases (Henry et al., 2012;Odum et al., 1996;Pathak et al., 2007). Changes to aerosol composition as a function of C_{OA} can be explained by gas/particle partitioning in which the distribution of material between the gas and particle phases is related to the saturation vapor concentration, C^*, and the total OA concentration (Pankow, 1994;Odum et al., 1996) according to:

$$\frac{C_{i,p}}{C_{i,tot}} = \alpha_i \left(1 + \frac{C_i^*}{C_{OA}}\right)^{-1} \quad (1)$$

where $C_{i,p}$ is the concentration of compound *i* in the particle phase (μg m^{-3}), $C_{i,tot}$ is the total concentration of *i* in both the gas and particle phase (μg m^{-3}), C^*_i is the saturation vapor concentration (μg m^{-3}) and α_i is the mass yield of compound *i*. When C_{OA} is equal to C^*_i 50% of compound *i* exists in the particle phase. Compounds are generally considered semi-volatile when their C^*_i are within 1-2 orders of magnitude of the concurrent C_{OA}. According to gas/particle partitioning, as C_{OA} increases the fraction of higher volatility compounds, which usually have a lower O/C ratio, present in the condensed phase will increase. SOA growth experiments have historically been interpreted through the framework of absorptive gas/particle partitioning theory, where volatility distributions, i.e. distributions of α_i as a function of C^*_i for some number of surrogate compounds, are derived by fitting the observed SOA formation (Odum et al., 1996;Donahue et al., 2006). Such analyses indicate that SOA is composed of a distribution of semi-volatile compounds with volatilities greater than ~ 10^{-1} μg m^{-3}. However, the volatility distributions determined from fitting of growth experiments have been mostly unable to describe the reverse process, namely evaporation of SOA. .

For example, quantitative estimates of the volatility of both ambient and laboratory OA after heating induced evaporation indicate that there are often components of OA with significantly lower volatility than predicted by fitting of growth experiments (Cappa and Jimenez, 2010;Stanier et al., 2007). In addition, several experiments have observed slower than expected room-temperature evaporation of both ambient (Vaden et al., 2011) and laboratory generated (Saleh et al., 2013;Grieshop et al., 2007;Wilson et al., 2015;Vaden et al., 2011), SOA during isothermal dilution. It has also been observed that the mass spectrum of α-pinene + O_3 SOA over the range 40-200 amu exhibited negligible changes during the heating induced evaporation (Cappa and Wilson, 2011), even though absorptive gas/particle partitioning suggests an SOA composed of components having volatilities spanning several decades of C^*. Some other experiments have observed some changes to the observed particle composition (i.e. mass spectrum) upon heating (Hall and Johnston, 2012b;Kostenidou et al., 2009), but overall the changes tend to be small and inconsistent with the particles being composed of individual compounds with a wide range of volatilities. Altogether these observations illustrate that there is a clear gap between the apparent volatility of SOA as characterized during evaporation experiments and the effective volatility of SOA derived from formation studies.

In this study, the volatility of α-pinene + O_3 SOA was characterized by heating-induced evaporation in a thermodenuder (TD) as a function of C_{OA} over the range 1 to 800 μg m^{-3}. Based on previous SOA formation experiments, the SOA composition is expected to have changed as C_{OA} was increased from 1μg m^{-3} to >140 μg m^{-3} (Shilling et al., 2009). It follows that the SOA volatility should vary as a function of C_{OA} as well, with an expectation that SOA at higher C_{OA} should be more volatile than that at low C_{OA} and thus should exhibit different responses to heating. Additionally, mass thermograms of SOA that was initially formed at C_{OA} >380 μg m^{-3} and rapidly diluted to C_{OA} < 30 μg m^{-3} were measured. The experimental results are interpreted using the kinetic model of aerosol evaporation in a TD by Cappa (2010) that has been extended from the original formulation that assumed direct evaporation of semi- or low-volatility monomers to include dimer formation and decomposition. Good agreement between the experimental observations and the model predictions provide support for the large influence of oligomer decomposition on SOA evaporation.

2 Materials and Methods

2.1 Secondary Organic Aerosol Production

SOA was formed in the absence of seed particles at various total C_{OA} from the formation and subsequent growth of nano-condensation nuclei~~homogeneous nucleation of~~ that were formed from products ~~produced from~~ of the ozonolysis of gas-phase α-pinene, in excess~~, in the absence of seed particles~~ (Fig. S1). Variable amounts of α-pinene were introduced into a stainless steel flowtube (L = 2 m; ID = 2.3 cm) by constantly injecting liquid α-pinene (0.12-0.7 μL h^{-1}) into a stream of purified house air at 0.015 lpm. The O_3 was generated by passing air through a cell containing a 22.9 cm long Hg pen-ray lamp (UVP, LLC.) and then 0.70-1.0 lpm of this flow was sub-sampled into the flowtube. The relative humidity of the air stream was ~30% for all experiments. The concentrations of α-pinene, O_3 and other experiment-specific conditions are given in Table 1. The residence time in the flow tube was typically about 1 minute, although slightly variable depending on the total volumetric flow rate (see Table 1). No OH scavenger was used. The O_3 concentration was measured using an O_3 Monitor (Model 450, API Inc.). Downstream of the flowtube residual hydrocarbons and O_3 were removed by passing the airstream through a Carulite 200 (Carus) catalyst and a charcoal denuder. The particles were assumed to have a density of 1.2 μg m^{-3}. The

particle mass concentrations were varied from 1 to 800 μg m^{-3} although were kept stable for the duration of each experiment. Larger concentrations tended to correspond to particle size distributions that peaked at larger sizes.

In addition to SOA that was generated at variable C_{OA}, seven experiments involved the dilution of SOA that was initially formed at high C_{OA} (≥380 μg m^{-3}) and diluted to low C_{OA}. The dilution occurred downstream of the flowtube, charcoal denuder and ozone denuder. To achieve the desired dilution the aerosol-laden airstream was divided into two fractions; one was directed through a HEPA capsule filter with Versapor® membrane (Pall Corp.) to remove particles from the air stream and the other passed directly through 1/8-in copper tubing. The two air streams were recombined after the filter and passed directly to the TD. The fraction of the airstream directed through the HEPA filter, i.e. the level of dilution, was controlled by a needle valve attached to the outlet of the filter.

2.2 Thermodenuder

The TD used here is based on the design of Huffman et al. (2008) with the following key modifications: 1) the heated laminar flow reactor is 0.71 m long (as compared to 0.41 m) and has a center line fully-heated residence time (τ_{res}) of 26 seconds at a flow rate of 0.40 lpm; 2) the distance between the actively heated volume and the charcoal denuder has been shortened and is now 4.8 cm (as compared to ~14 cm); 3) there is only one heating region. The shorter distance between the end of the actively heated volume and the charcoal denuder helps to limit re-condensation as the air cools prior to reaching the denuder section. The bypass (i.e. unheated) line had the same volume as the TD, and thus the same total residence time. Further information on the design and characterization of the TD is provided in the *Supplemental Information*. The room temperature flowrate through the TD was a constant 0.40 lpm independent of the total flowrate in the SOA formation flowtube. Measurements of the particle size distribution were made after the particles passed through either the bypass line (room temperature) or the TD. The TD temperature ranged from room temperature (298 K) to 220°C (493 K). No differences in the mass thermograms were found between experiments based on the order of temperature changes, e.g. whether temperature was increased or decreased.

2.3 Measurements

A scanning mobility particle sizer (SMPS; TSI, Inc.), composed of a charge neutralizer, a differential mobility analyzer (DMA; Model 3085) and a condensation particle counter (CPC; Model 3772), was used to measure particle size distributions. The extent of aerosol evaporation was characterized by comparing the particle size distribution for particles that passed through the bypass line to that for the particles after passing through the TD. The size distributions were characterized by their volume-weighted median diameter, $d_{p,V}$. The particle volume fraction remaining (VFR) after passing through the TD is then:

$$VFR = \frac{\frac{\pi}{6} d_{p,V,TD}^3}{\frac{\pi}{6} d_{p,V,bypass}^3}, \quad (2)$$

where $d_{p,V,TD}$ and $d_{p,V,bypass}$ refer to the particles that passed through the TD or the bypass, respectively. Under an assumption of constant particle density, the VFR is equivalent to the particle mass fraction remaining (MFR), and plots of VFR versus temperature are commonly referred to as mass thermograms. The bypass distribution was measured at least every two temperature changes (~every 20 minutes) to account for any changes in the reference particle distribution; in general, the reference distributions were very stable.

To facilitate quantitative comparison between experiments at different C_{OA}, each mass thermogram was fit to the sigmoidal type equation from Emanuelsson et al. (2013):

$$VFR(T) = VFR_{max} + \left(\frac{VFR_{min} - VFR_{max}}{1 + \left(\frac{T_{50}}{T}\right)^{S_{VFR}}} \right), \quad (3)$$

where VFR_{min} is the VFR at the low temperature limit, VFR_{max} is the VFR at the high temperature limit (typically zero), S_{VFR} is the slope factor that characterizes the steepness of the VFR curve and T_{50} is the temperature at which VFR = 0.50. If there is no evaporation in the TD at room

temperature due to the removal of gas-phase compounds (vapor stripping) in the denuder section then the VFR at room temperature (298 K) should be, by definition, unity. Best-fit VFR_{min} values greater than unity may, however, be obtained because Eqn. 3 is an empirical expression and thus is not expected to provide a perfect match with the observations, although can nonetheless facilitate comparison between different experiments. Here, to provide for more consistent fitting and since no evaporation was observed at room temperature ~~was observed~~, the fit curves were forced to go through unity at room temperature.

2.4 Kinetic Model of Evaporation

2.4.1 Thermodenuder model

The kinetic model of evaporation used here is a modified version of the model developed by Cappa (2010) to simulate evaporation in a thermodenuder. The original model simulated gas/particle mass transfer (evaporation and condensation) for a monomodal multi-component aerosol as particles pass through and are heated and cooled in the TD along with loss of vapors to the charcoal denuder. Absorptive partitioning is implicitly assumed. Compounds evaporate according to their respective saturation vapor concentrations, and it is assumed that the gas/particle system is at equilibrium before entering the TD. The temperature dependence of C^* is accounted for using the Clausius-Clapeyron equation. Here, it is assumed that the enthalpy of vaporization, ΔH_{vap}, is related to C^* according to the relationship of Epstein et al. (2010), where ΔH_{vap}(kJ mol^{-1}) = 131 - 11×log C^*. The temperature profile through the TD is empirically specified (see SI). The key input to the model is the distribution of mass (gas + particle) with respect to C^*, referred to as a volatility distribution; different distributions will yield different mass thermograms (Cappa and Jimenez, 2010). It is commonplace to assume a distribution where the C^* values differ by an order of magnitude at a specified reference temperature, e.g. log C^*(298 K) = (-3, -2, -1, 0, 1, 2, 3), and this approach is adopted here. The calculated mass transfer rates can be adjusted to account for mass transfer limitations, as characterized by the evaporation coefficient, γ_e, which characterizes deviations from the theoretical maximum evaporation rate; γ_e is an adjustable parameter as it is not known *a priori*. The default value used is $\gamma_e = 1$. The model output for a given set of ΔH_{vap} and C^* is dependent on γ_e. At smaller γ_e the slope of the mass thermogram is less steep, the T_{50} increases and for SOA with semi-volatile components an increasing amount of mass remains after TD-processing at room temperature (Cappa and Wilson, 2011). The model can be run with pre-

specified volatility distributions or can be used to determine empirical volatility distributions from fitting to observations (Cappa and Jimenez, 2010).

The base TD model has been modified to include the influence of dimers and dimer decomposition on the simulated evaporation, and shares some similarities with Trump and Donahue (2014). The dimer model is implemented as follows. The initial equilibrium gas/particle mass distribution is based on a semi-volatile monomer volatility distribution (i.e. that determined from previous growth experiments). The balance between monomers and dimers at equilibrium is then determined from the monomer/dimer equilibrium constant, K_{eqm} (cm^3 $molecules^{-1}$), which is equal to the ratio of the forward (k_f, cm^3 $molecules^{-1}$ s^{-1}) and reverse (k_r, s^{-1}) rate coefficients associated with formation from monomers and dimer decomposition, i.e. $K_{eqm} = k_f/k_r$. Note that the volume units on K_{eqm} and k_f correspond to condensed-phase volume. If K_{eqm} is large then all condensed-phase species would be in dimer form and, at equilibrium, all gas-phase material would be drawn into the condensed phase, assuming that the monomers are miscible with the dimers. Here, this situation is avoided through the following simplification to determine the initial particle state at the TD inlet. First, the gas/particle (monomer only) equilibrium distribution is calculated given the specified volatility distribution and C_{OA}. Then the monomer/dimer equilibrium in the condensed phase only is calculated based on the current condensed-phase monomer concentrations. The ~~, and the~~ gas-phase concentrations are then set to zero to avoid large amounts of condensing material at the next time step. Since a charcoal denuder is placed immediately after the flowtube, this simplification is physically ~~accurate~~reasonable as we have previously found that vapor stripping in charcoal denuders is efficient (Cappa and Wilson, 2011). The resulting ~~gas-~~monomer-dimer concentrations in the condensed phase are used as the initial state. The above simplification for the initial particle state most likely does not provide a true representation of the actual particle composition, just as the assumption regarding only homodimers (discussed below) is a simplification. However, as we ultimately find that the simulation results are much more sensitive to the initial distribution of particulate mass with respect to monomers and dimers than to the specific distribution of monomers with respect to their volatility, these simplifications will influence the details but not the general conclusions arrived at here.

It is assumed that the dimers are non-volatile over the entire temperature range considered, and thus do not directly evaporate. In addition, only homodimers, that is dimers formed from

monomers in the same volatility bin, are assumed to form. This is a simplification compared to allowing for all possible cross-reactions and allows for more straight-forward keeping track of the dimer source monomers. As the temperature increases within the TD the dimers decompose into their semi-volatile parent monomers, which can then evaporate according to their saturation vapor concentration. It was assumed that there were no mass transport limitations within the particle-phase for all evaporating species, i.e. that the surface composition was always equivalent to the bulk composition. As the semi-volatile monomers evaporate the equilibrium state is perturbed and the dimers decompose in response, according to the temperature dependent K_{eqm}, to re-establish dimer/monomer equilibrium. Depending on the timescale of dimer formation and decomposition, the dimers and monomers may not be in equilibrium at every step of the model, yet they are constantly forming and decomposing to move towards equilibrium. Experimental observations by Hall and Johnston (2012b) have shown that dimers in SOA do decompose upon heating. The rate at which dimers decompose is governed by changes to k_r and k_f, ~~both of which are likely to be~~ as a function of temperature ~~dependent~~. Assuming they exhibit Arrhenius-type temperature dependence, the temperature sensitivity of K_{eqm} can be characterized by the difference in the activation energies of the reverse and forward reactions, $\Delta E_a = E_{a,r} - E_{a,f}$, and where the temperature dependence of k_r and k_f has the form:

$$k_r(T) = k_r(298K) \cdot e^{\left(-\frac{E_{a,r}}{RT}+\frac{E_{a,r}}{R\cdot 298K}\right)} = A_r \cdot e^{-\frac{E_{a,r}}{RT}} \quad (4)$$

where R is the universal gas constant (8.314 J mol^{-1} K), T is the temperature (K) and where

$$A_r = k_r(298K) \cdot e^{-\frac{E_{a,r}}{R\cdot 298}}. \quad (5)$$

Note that the Arrhenius pre-factor, A_r, depends on $E_{a,r}$. Consequently,

$$K_{eqm}(T) = \frac{k_r(298K)}{k_f(298K)} \cdot e^{-\frac{\Delta E_a}{R\cdot 298K}} \cdot e^{-\frac{\Delta E_a}{RT}} = \frac{A_r}{A_f} \cdot e^{\frac{\Delta E_a}{RT}} \quad (6)$$

and ΔE_a is as defined above. It should be noted that this formulation differs somewhat from that of Trump and Donahue (2014) in that they assumed that A and E_a were independent parameters and further did not account for the T-dependence of k_f, which we account for here in the relationship between k_r, k_f and ΔE_a. The key model inputs are then K_{eqm}(298 K), k_r(298 K) and ΔE_a. Although K_{eqm} governs the equilibrium distribution, k_f and k_r will control the timescales associated with dimer formation and the approach to equilibrium in the particles.

2.4.2 Isothermal evaporation model

The kinetic thermodenuder model of evaporation was adapted to allow for simulation of particle evaporation at room temperature following from isothermal dilution for any initial input of particle composition including semi-volatile monomers, very low volatility compounds and a mixture of semi-volatile monomers and non-volatile dimers. The extent of dilution is user-selectable as a dilution factor (DF), which simulates SOA and the associated vapors being passed through a DMA and injected into a chamber. The organic vapors are assumed to be removed from the system (i.e. lost to the chamber walls) with a rate characterized by a user-selectable first order loss rate, k_{loss} (s^{-1}). Vapor loss serves to mimic the conditions in some isothermal evaporation experiments where the diluted SOA particles are held in a chamber containing activated carbon (Vaden et al., 2011). The timescales associated with isothermal evaporation are much longer than for the TD experiments and simulations, and the isothermal evaporation model can be run for many hours of model time. When the monomer/dimer equilibrium is used to establish the initial particle composition, the relationships between K_{eqm}, k_r, k_f and ΔE_a are the same as in the TD evaporation model.

3 Results and Discussion

3.1 Observations

Evaporation and shrinking of the α-pinene+O_3 SOA particles occurred upon heating in the TD. Example size distributions as a function of temperature for an initial C_{OA} = 9 μg m^{-3} are shown in Figure 1. The mass thermograms for each individual experiment are shown in Figure 2. The experimental results have been grouped according to the bypass C_{OA} for each experiment, with

groupings of: (i) high, C_{OA}>300 μg m^{-3}; (ii) medium, 90≤C_{OA}<300 μg m^{-3}; and low, C_{OA}≤30 μg m^{-3}. The demarcations were chosen based on the results from Shilling et al. (2009), who observed that particle composition varied with C_{OA}. Results from experiments where SOA was formed at a high C_{OA} (>300 μg m^{-3}) and then rapidly isothermally diluted to a lower concentration (<30 μg m^{-3}) are also reported in Figure 2. Each experiment was individually fit according to Eq. 3, and the best-fit parameters are given in Table S1. The average T_{50} and S_{VFR} for each C_{OA} grouping are given in Table 2.

Within each grouping the mass thermograms are all very similar, especially for the low and medium cases. No evaporation is observed at room temperature from vapor stripping in the denuder section for any case. The maximum variability is observed within the high C_{OA} grouping, although even here the variability is not particularly large, with the average and sample standard deviation S_{VFR} = 16.4 ± 1.5 and in T_{50} = 359 ± 7K. The S_{VFR}'s for all groupings are statistically indistinguishable, as are the T_{50} values for the low and medium groupings. However, the T_{50} for the high C_{OA} grouping is significantly larger at the $p < 0.05$ level ($p = 0.006$ and $p= 0.025$ as compared to the low and medium C_{OA} groupings, respectively, for a two-tailed test). Visual inspection of Figure 2a indicates that one experiment, with C_{OA} = 600 μg m^{-3}, has a notably larger T_{50}. If this experiment is excluded the T_{50} = 357 ± 5 K, which is still statistically larger than the low C_{OA} T_{50} at the $p<0.05$ level ($p = 0.008$ for the two-tailed test) but is only now statistically larger than the medium C_{OA} T_{50} at the $p<0.10$ level ($p = 0.079$ for the two-tailed test). This difference could be due to small amounts of re-condensation or to saturation of the gas-phase, both of which become a greater concern at high C_{OA} (Cappa, 2010;Saleh et al., 2011;Cappa and Jimenez, 2010;Fuentes and McFiggans, 2012;Riipinen et al., 2010), although there is no specific dependence of T_{50} on C_{OA} within the high C_{OA} group. Regardless, it is apparent that the effective volatility of the SOA at high C_{OA} is not higher than at low C_{OA} and that, despite the slight differences, the response to heating of SOA particles formed from products of the ozonolysis of α-pinene is, to a very large extent, independent of the C_{OA} at the point of formation. This then suggests that, from a volatility perspective, the distribution of compounds in the particle is independent of C_{OA}, which stands in contrast to expectations based on the growth-derived volatility distribution.

The mass thermogram of SOA originally formed at high C_{OA} and isothermally diluted to low C_{OA} was also measured (Figure 2d). Since the evaporation of SOA induced by isothermal dilution occurs very slowly, on the order of many minutes to hours (Grieshop et al., 2007;Saleh et al., 2013), the composition of the diluted SOA is not expected to change substantially from the initial state of formation at high C_{OA} before the particles enter the TD. The T_{50} of the SOA formed at high C_{OA} is larger than for the diluted SOA, and significantly different at the $p < 0.05$ level ($p = 0.003$ for a two-tailed test), while the average S_{VFR} of the diluted and the high C_{OA} grouping mass thermograms are statistically indistinguishable at the $p<0.05$ level ($p = 0.443$ for the two-tailed test). This strongly suggests that the difference in T_{50} of the high C_{OA} grouping results from re-condensation or saturation of the gas-phase, although the possibility that there is some real difference in the effective volatility of particles after rapid isothermal dilution cannot be excluded. The average diluted SOA mass thermogram is also almost identical to the average low C_{OA} mass thermogram indicating that the volatility distributions of the compounds in the diluted and low C_{OA} cases are the same. Overall, it is evident that the rapid dilution of SOA does not induce changes to molecular composition that significantly influence particle volatility.

3.2 Evaporation Modeling

3.2.1 Semi-volatile SOA model

The observed similarity between the mass thermograms for the SOA formed at orders of magnitude different C_{OA} is surprising given that some observations suggest that particle composition depends on C_{OA} (e.g. Shilling et al. (2009)). Since the application of absorptive partitioning theory to the interpretation of SOA growth experiments suggests that the particles are (i) composed of compounds with a large distribution of individual volatilities, typically with C^* values $> 10^{-1}$ μg m^{-3} and (ii) that the fraction of higher volatility compounds should increase with increasing C_{OA}, the mass thermograms are expected to depend on C_{OA}. Using a volatility distribution for α-pinene + O_3 SOA derived from SOA formation experiments (Pathak et al., 2007), simulated mass thermograms have been calculated as a function of C_{OA} (for $\gamma_e = 1$ or 0.001) using the TD model, first assuming that the particles are composed only of monomers (Figure 3). Results from this model will be referred to as semi-volatile monomer results. Specifically, we use the 7-bin volatility distribution with $\log C^* = [-2,-1,0,1,2,3,4]$ and mass yields of $\alpha = [0.001, 0.012, 0.037, 0.088, 0.099, 0.250, 0.800]$. The theoretical mass thermograms, for $\gamma_e = 1$, indicate that a

significant dependence of the mass thermograms on C_{OA} should have been observed (Figure 3a). Further, they indicate that substantial evaporation of the SOA particles at high C_{OA} should have been observed at room temperature due to vapor stripping in the charcoal denuder section of the TD, which occurs to some extent for any species with $C^* \geq \sim 1$ μg m^{-3} when $\gamma_e = 1$. Neither of these phenomena were observed, demonstrating that there is a clear disconnect between typical volatility distributions derived from SOA growth experiments and SOA evaporation experiments, as has previously been noted (e.g. (Cappa and Jimenez, 2010)).

Some measurements of time-dependent evaporation profiles of SOA have been interpreted as suggesting that γ_e is significantly less than unity for α-pinene + O_3 SOA due to mass transfer limitations in the condensed phase (Grieshop et al., 2007;Saleh et al., 2013;Karnezi et al., 2014). Further, some TD-based SOA studies have used γ_e as a tunable parameter in data fitting for individual experiments and suggest that $\gamma_e < 1$ (Lee et al., 2011;Lee et al., 2010). Therefore, model predictions for C_{OA} dependent mass thermograms are also reported for $\gamma_e = 0.001$ (Figure 3b). As expected, the apparent volatility (i.e. extent of evaporation at a given temperature) is decreased compared to the $\gamma_e = 1$ case, and the simulated thermograms exhibit a greater similarity to the observations. Also, the extent of evaporation at room temperature is substantially lowered and more consistent with the observations, as now only species with $C^* \geq \sim 1000$ μg m^{-3} will evaporate to any substantial extent in the TD due to vapor stripping alone. However, the simulations also indicate a very strong C_{OA} dependence — higher volatility with higher C_{OA} — is expected when $\gamma_e = 0.001$, which is inconsistent with the observations here. This demonstrates that conclusions regarding the magnitude of parameters such as γ_e when derived from single experiments may not provide a robust description of the process in question (here, evaporation) because they are not unique solutions (i.e. are dependent on the other model inputs, namely the assumed ΔH_{vap} and volatility distribution). Regardless of assumptions about mass transfer limitations, the model predictions for the mass thermograms of particles comprised entirely of monomers (i.e. based on the Pathak et al. (2007) volatility distribution) unambiguously show a dependence on C_{OA}. Thus, there is a clear disconnect between volatility distributions derived from SOA growth experiments and observations from SOA evaporation experiments that cannot be entirely explained by kinetic limitations to evaporation.

3.2.1 Dimer-Decomposition Model

The above discrepancy strongly suggests that the molecular composition of the condensed phase is only indirectly related to the volatilities of the condensing species as determined from growth experiments. Here, the possibility that this discrepancy can be explained through the formation and subsequent decomposition of dimers (and higher-order oligomers) through condensed phase reactions is examined. Cappa and Wilson (2011) demonstrated that, although simple applications of equilibrium absorption partitioning theory can explain SOA growth in laboratory chamber experiments, such models are not unique explanations. In particular, they showed it was possible to reconcile SOA growth experiments with the occurrence of condensed-phase reactions—even to the extent that the entire particle is rapidly converted from monomers (that retain the volatility of the condensing species) to non-volatile species. There is now a variety of experimental evidence that many types of SOA particles are composed of a large fraction of oligomers (Kourtchev et al., 2014;Putman et al., 2012;Kundu et al., 2012;Gao et al., 2004a;Muller et al., 2009;Kalberer et al., 2004), which will generally have volatilities lower than the monomeric precursors. For the system considered in this study, α-pinene + O_3 SOA, the oligomeric content is suggested to be greater than 50% (Tolocka et al., 2004;Gao et al., 2004a;Gao et al., 2004b;Hall and Johnston, 2012a) and both laboratory (Kristensen et al., 2014) and ambient (Kristensen et al., 2013;Yasmeen et al., 2010) measurements have identified several α-pinene+O_3 SOA dimers.

Simulated mass thermograms have been calculated as a function of C_{OA} using the modified TD model, in which some fraction of the condensed-phase material is assumed to exist as dimers. The same 7 volatility bins were used with the same mass yields as the semi-volatile monomer case to calculate the initial concentration of monomers in the particle. As described above, the equilibrium coefficient, K_{eqm}, was used to determine the initial monomer/dimer equilibrium while the decomposition rate coefficient, k_r, and activation energy, ΔE_a, describe the rate and sensitivity to temperature changes of dimer thermal decomposition. None of the parameters are known *a priori*. Since there is a relationship between all three parameters ($K_{eqm} = k_f/k_r$ and $k_r(T)$ are dependent on ΔE_a) we have taken the approach of specifying different values of K_{eqm} and then fitting the model to the observations by adjusting k_r and ΔE_a. The level of model/measurement agreement for the different K_{eqm} was then assessed.

The model aerosol used had d_p = 90 nm and C_{OA} = 100 μg m^{-3} as starting conditions, and was fit to the average mass thermogram of the medium/low C_{OA} grouping (Figure 4a). Generally good

fits were obtained for all K_{eqm} over the range 10^{-18} to 10^{-14} cm^3 molecule^{-1}, with the overall best agreement obtained for $K_{eqm} = 10^{-17}$ cm^3 molecule^{-1}, although the differences are quite small (see the *SI* for the best-fit model parameters for each K_{eqm}). At smaller K_{eqm}, extensive room temperature evaporation occurred as a result of the increasing initial fraction of semi-volatile monomers, a result that is inconsistent with the observations. However, even for the simulations at larger K_{eqm}, some evaporation at room temperature was always predicted. The simulated room temperature evaporation at larger K_{eqm} may result from the model assumption of liquid-like particles in that if mixing within the particles were slow such that there were a build up at the particle surface of non-volatile dimers then evaporation of monomers that are buried below the surface would be slowed (Roldin et al., 2014). The associated best fit k_r(298 K) and ΔE_a varied with K_{eqm}, from 1.6 x 10^{-3} s^{-1} to 2.8 x 10^{-2} s^{-1} and from 15 kJ/mol to 42 kJ/mol, respectively; smaller K_{eqm} values corresponded to larger k_r and smaller ΔE_a.

These K_{eqm} values correspond to a case where the particles are almost entirely composed of dimers, as the dimer fraction is >97% for all $K_{eqm} > 10^{-18}$ cm^3 molecule^{-1}. The range of best-fit k_r indicate a dimer lifetime of only 1-10 minutes with respect to decomposition at room temperature. The range of k_f values associated with the best fit K_{eqm} and k_r is 1.6 x 10^{-21} to 2.8 x 10^{-16} cm^3 molecules^{-1} s^{-1}. Given a typical molecular density of ~10^{21} molecules cm^{-3}, the approximate dimer formation timescale is only a fraction of a second, consistent with the short reaction time in these experiments. Consequently, the dimer decomposition timescale is not the same as the observable timescale associated with particle mass loss at room temperature upon e.g. isothermal dilution (Grieshop et al. (2007)). However, there are several potential factors that slow down evaporation at room temperature despite the short dimer lifetime with respect to decomposition, as discussed below when isothermal dilution and evaporation is considered. The K_{eqm}, k_r, and ΔE_a determined above from fitting the medium/low C_{OA} data (i.e. C_{OA} = 100 μg m^{-3}) have been used to predict additional mass thermograms for C_{OA} = 1, 10, 70 and 600 μg m^{-3} (Figure 5a). The predicted mass thermograms are mostly independent of C_{OA}, in contrast with the semi-volatile monomer model. Thus, when the particle is nearly entirely initially dimers this "dimer-decomposition" model result is generally consistent with the experimental observations, where limited differences were observed between the mass thermograms measured at different C_{OA}, although it should be noted the slight increase in T_{50} observed at the highest mass loadings is not reproduced. Also, only the

C_{OA} = 1 μg m^{-3} simulation predicts negligible evaporation at room temperature, as was observed for all C_{OA}. The dimer-decomposition model also predicts that the observable particle composition should remain relatively constant as evaporation is induced (Figure 6a), consistent with observations. This prediction is consistent with previous measurements in which it was observed that the particle composition, as measured using a vacuum ultraviolet aerosol mass spectrometer (VUV-AMS) remained quite constant during the heating induced evaporation of α-pinene+ O_3 SOA (Cappa and Wilson, 2011). There are several experiments where changes to composition were observed. Hall and Johnston (2012b) used an electrospray ionization Fourrier transform ion cyclotron resonance (ESI-FTICR) mass spectrometer to measure the fraction of oligomers in the particle before and after heating (393 K) and found that the fraction of oligomers and the O:C ratio increase after heating. Furthermore, when re-condensation does occur, the compounds that recondensed appear to be monomer decomposition products. Kostenidou et al. (2009) used a quadropole AMS to quantify the mass fraction of *m/*z 44 fragments as a function of MFR and found that the fraction of *m/*z 44 increased as MFR decreased, indicating more oxygenated particles with heating-induced evaporation. Since the dimer model presented here tracks the relative concentration of dimers and monomers due to decomposition, the most comparable study is Cappa and Wilson (2011) because the measurement technique is one that primarily detects the monomer components due, most likely, to thermal degradation during analysis.

Trump and Donahue (2014) and Roldin et al. (2014) have previously suggested that accounting for the behavior of dimers within SOA can help to explain observations of SOA evaporation; our observations and analysis support and expand upon this conclusion. The range of k_r independently determined here are somewhat larger than the room-temperature k_r suggested by Trump and Donahue (2014) (=1.1x10^{-4} s^{-1}) and Roldin et al. (2014) (=2.8x10^{-5} s^{-1}), which were based on needing an evaporation timescale of ~1 hr for isothermal evaporation (Grieshop et al., 2007;Vaden et al., 2011). Ultimately, reconciliation of the different timescales indicated for dimer decomposition between the different studies likely will require more detailed consideration of the exact nature of various dimer types with respect to their decomposition and formation timescales, which may not all be identical as assumed here, and of the influence of particle phase on evaporation.~~However, their estimates may not have fully accounted for the dynamic nature of the system, and thus underestimated the actual dimer decomposition rates compared to that obtained here.~~ It should be noted that the ΔE_a determined here are substantially smaller than that suggested

by Trump and Donahue (2014), who give $E_{a,r}$ ~80 kJ mol^{-1} (and where, it seems, that their $E_{a,r}$ is essentially equal to the ΔE_a here as they assume that k_f is T-independent). However, this difference can be understood by recognizing that they assumed a constant value for A (= 3 x 10^{10} s^{-1}) and k_r(300 K) and determined $E_{a,r}$ using the relationship $k_r(T) = A\exp(-E_{a,r}/RT)$. Thus, underestimations of k_r may lead them to actually overestimate the true temperature sensitivity of the system.

The best-fit K_{eqm} and k_r were determined from fitting to T-dependent evaporation experiments that occur over relatively short timescales (~1 min) in the thermodenuder. To facilitate more direct connections with previous experiments that have investigated room temperature evaporation upon dilution, the best-fit dimer-decomposition model for K_{eqm} = 10^{-17} cm^3 molecules^{-1} has been used to simulate the long-time, isothermal, room-temperature evaporation of SOA for the case where the SOA is initially diluted and the evaporating vapors are constantly being stripped from the gas-phase (Figure 4b). This corresponds approximately to the conditions in a series of experiments investigating SOA evaporation (Vaden et al., 2011;Wilson et al., 2015). A vapor loss rate constant of k_{loss} = 10^{-3} s^{-1} has been used, which is a reasonable estimate given the size of the chambers used in the previous experiments (Matsunaga and Ziemann, 2010;Zhang et al., 2014). The initial (pre-dilution) C_{OA} = 100 μg m^{-3}, which was diluted by a factor of DF = 30 to induce evaporation.

The literature experiments have generally shown evidence for evaporation of SOA on fast, medium and slower timescales, where "fast" corresponds to timescales of around a minute, "medium" corresponds to timescales of around 1 hour and "slow" to timescales of many hours. The dimer model simulations for all the K_{eqm} fits exhibit similar behavior, with "fast," "medium" and "slow" periods of mass loss and timescales similar to previous observations. There is a non-monotonic dependence on K_{eqm}, with the least mass loss predicted for K_{eqm} = 10^{-16} cm^3 molecules^{-1} and greater total mass loss predicted for K_{eqm} both larger and smaller. The behavior results from a balance between the k_r, k_f and evaporation time scales for each K_{eqm} fit. After 15 h the simulated MFR of SOA is 5-27% of the initial (post-dilution) C_{OA}. The general model behavior, which indicates that evaporation occurs on multiple timescales, can be understood by recognizing that decomposition of dimers composed of higher C^* monomers leads to rapid evaporation, such that the observable evaporation rate is controlled by the dimer decomposition. In contrast, decomposition of dimers composed of lower C^* monomers results in species that do evaporate, but only slowly at room temperature. Given a distribution of monomers with respect to their C^*,

the result is a time-dependent evaporation profile multiple apparent timescales for evaporation. Further, as evaporation proceeds, the finite rate of vapor loss means that over time the gas-phase concentration may build up, which will also limit the rate of mass loss.

The simulated MFR values at the end of 15 h of SOA evaporation are somewhat lower than was observed in the literature experiments for dry, fresh SOA from α-pinene + O_3, where MFR ~ 0.35-0.4 at 15 h (Vaden et al., 2011;Wilson et al., 2015). However, the extent of evaporation is dependent on the model assumptions, specifically the k_{loss} and *DF*. Smaller k_{loss} or *DF* leads to larger MFR at a given time due to more extensive inhibition of evaporation resulting from faster saturation of the gas-phase (Figure 7a). Conversely, larger k_{loss} or *DF* lead to more extensive evaporation. As neither the k_{loss} nor *DF* are explicitly known for the literature experiments, a more quantitative comparison is not possible. However, it is nonetheless noteworthy that the model suggests that both k_{loss} and *DF* can play a controlling role in observations of isothermal evaporation. These previous isothermal evaporation measurements also indicate that SOA evaporation is mostly size independent, in contrast to evaporation of single-component particles (Vaden et al., 2011;Wilson et al., 2015). Simulations using the dimer-decomposition model with different starting particle sizes show some dependence on particle size (d_p = 90, 180 and 360 nm), with larger particles having smaller MFRs at a given time (Figure 7a). However, the overall differences are relatively small and reasonably consistent with the observations given that the observations have typically considered a narrower size range than examined here.

3.2.1 Low-volatility SOA Model

One alternative possibility to explain the observations of evaporation of SOA in the TD is that the observed heating-induced evaporation results from direct evaporation of low-volatility species. These low-volatility species could be either highly oxygenated monomers (Ehn et al., 2014) or thermally-stable dimers or higher-order oligomers, although the thermal stability of dimers seems unlikely (Hall and Johnston, 2012a). To test this idea, the TD model has been fit to the observations assuming that the particles are only composed of semi- and low-volatility species, but where the volatility distribution is skewed to much lower C^* than suggested from SOA growth experiments (i.e. from the Pathak et al. (2007) volatility distribution). Given that there is negligible evaporation observed at room temperature in the TD for all C_{OA}, including C_{OA} = 1 μg m^{-3}, the highest volatility bin was set at C^* = 1 μg m^{-3}. The lowest value was set based on the requirement that there remains

some particle mass at ~343 K. If ΔH_{vap} is too large then even very low-volatility compounds will not persist to such high temperatures (Cappa and Jimenez, 2010;Cappa, 2010). As such, an upper-limit ΔH_{vap} constraint of 185 kJ mol^{-1} was placed on the $C^*/\Delta H_{vap}$ parameterization, and a lower bound C^* of 10^{-9} μg m^{-3} was used. Following Cappa and Jimenez (2010), a relationship between the total organic mass and C^* was assumed, where $C_{i,tot} = a_1 + a_2\exp[a_3(\log(C^*)+a_4)]$. Values of the a_x parameters have been determined through data fitting; it is difficult to constrain the absolute C_{OA} while determining the a_x parameters through fitting, and thus C_{OA} was allowed to vary. The model was fit to the average thermogram for the medium/low C_{OA} grouping, and a good fit was found when the a_x = [1.53,8.5,0.3,0.59], with a corresponding C_{OA} of 71 μg m^{-3} (Figure 4a). This demonstrates that an alternative model can potentially be used to explain the TD results, namely one in which the condensed-phase species are very low volatility but evaporate directly in response to heating.

If the same a_x distribution is used, but with $C_{i,tot}$ scaled up or down to give a different initial C_{OA} (and slightly different distribution of compounds), the simulated volatility decreases slightly as C_{OA} increases (Figure 5b). This is mostly due to gas-phase saturation at higher concentrations, and subsequently greater re-condensation as the SOA cools in the denuder. Nonetheless, this is opposite the C_{OA} dependence predicted by the semi-volatile monomer model and is in the same direction of the observations, where the high C_{OA} grouping exhibited lower apparent volatility. There is, however, some difference in the simulated mass thermograms for low and medium C_{OA}, which was not observed, although the gap between the low (1-10 μg m^{-3}) and medium (100 μg m^{-3}) C_{OA} simulations is smaller than the gap between the medium and high (600 μg m^{-3}) C_{OA} simulations. If re-condensation of the evaporated species were, for some reason, not particularly efficient (due perhaps to changes in the molecular composition upon heating) then the differences between the different C_{OA} simulations would be lessened.

As with the dimer-decomposition model, simulation of isothermal evaporation by the low-volatility monomer model provides evidence for multiple evaporation timescales, with "fast," "medium" and "slow" components (Figure 4b). For the same k_{loss} (= 10^{-3} s^{-1}) and DF (= 30), the extent of evaporation from the low-volatility aerosol simulation at 15 h is less than for the various dimer-decomposition simulations. The low-volatility aerosol model exhibits a similar sensitivity to the assumed k_{loss} and DF, and a slightly smaller sensitivity to changes in particle size (Figure

7b). It is apparent that the low-volatility aerosol model is compatible with the observations from both our TD and the literature isothermal evaporation experiments (Vaden et al., 2011;Wilson et al., 2015).

Although both the low-volatility aerosol and dimer-decomposition models perform equally well in explaining the observed mass thermograms and literature observations of isothermal evaporation, there is a distinct difference between two model results in terms of how the particle composition is predicted to vary with temperature. Unlike the dimer-decomposition model, the predicted relative particle composition undergoes substantial changes as the particles evaporate upon heating for the low-volatility aerosol model (Figure 6b). This model result would suggest that potentially large changes in composition should be observed upon heating or, more generically, evaporation. This prediction is inconsistent with the various observations that suggest negligible to very moderate changes in the observed particle composition (Cappa and Wilson, 2011;Kostenidou et al., 2009).

3.2.1 Comparison between model results

Overall, the dimer-decomposition model of evaporation provides the most comprehensive explanation in that it can explain not only the current results where the observed mass thermograms are nearly independent of C_{OA}, but also the minor changes in composition that occur upon heating-induced evaporation of α-pinene+O_3 SOA observed by some (Cappa and Wilson, 2011), the moderately long timescales required for achieving equilibrium upon isothermal dilution (Grieshop et al., 2007) and the bimodality of SOA evaporation upon rapid dilution and subsequent continuous vapor stripping (Vaden et al., 2011). The low-volatility monomer evaporation model can reproduce many of these observations, but suggests large compositional changes upon heating. The semi-volatile monomer model fails to reproduce nearly all of the observations. Additionally, the dimer-decomposition model is potentially consistent with suggestions that SOA particles formed under dry conditions have very high viscosity (Kannosto et al., 2013;Virtanen et al., 2010;Abramson et al., 2013). The viscosity of SOA should decrease rapidly as temperature increases and, to the extent that SOA might actually be a glass, could go through a glass-liquid transition (Koop et al., 2011). If the particles were primarily semi-volatile monomers for which evaporation were limited by diffusion in the particle phase, then decreases~~changes~~ in viscosity should lead to substantial increases in the observed evaporation rate (Zaveri et al., 2014;Roldin et al., 2014). The continuous

change in VFR with temperature out to relatively high temperatures suggests that the condensed-phase species must have low-volatility such that as the viscosity decreases there is no substantial impact on the observed particle evaporation. This model/observation comparison suggests that for SOA—at least that produced from the α-pinene+O_3 reaction—the mass thermogram does not give direct information on the distribution of volatilities of the original condensing compounds (i.e. the monomers), but on the properties of the oligomers, specifically their thermal stability. One limitation of the current kinetic model is the assumption that k_r and ΔE_a are the same for all dimers, whereas it is likely that the rate and temperature-sensitivity of oligomer decomposition is compound specific (Hall and Johnston, 2012b). However, expansion of the model to include such information would only add more tunable parameters, but would not materially influence the conclusions here.

Despite the general success of the dimer-decomposition model in reproducing a variety of observations, it does predict some particle evaporation at room temperature in the TD, which was not observed. Further, it seems unlikely that all particle mass is converted to dimers on such rapid timescales as implied by the dimer-decomposition model; although accurate quantification of the relative fractions of dimers (and larger oligomers) versus monomers in SOA particles has proven challenging, it seems likely that the oligomer fraction is not 100% (Hall and Johnston, 2012b;Kalberer et al., 2004;Kristensen et al., 2014), some experiments have observed apparent variations in VFR, determined from either heating or vapor stripping, as the particles are "aged" by sitting in the dark (Abramson et al., 2013) or by exposure to oxidants (Kalberer et al., 2004;Salo et al., 2011;Emanuelsson et al., 2013), suggesting that compositional changes (including dimer or oligomer formation) may occur on multiple timescales, ranging from seconds to minutes to hours. It therefore seems likely that a more complete representation of α-pinene+O_3 SOA volatility is some hybrid of the dimer-decomposition and low-volatility species frameworks, where some substantial fraction of the condensed phase mass exists as very low-volatility, effectively non-volatile, dimers or oligomers — or even thermally-unstable, low-volatility monomers — that decompose to produce species with a distribution of volatilities that subsequently evaporate, while some fraction exists as low-volatility ($C^* < 1$ μg m^{-3}) species that can directly evaporate but for which the actual volatilities tend to be lower than those predicted from traditional analyses of growth experiments. Regardless of the details, the effective volatility of α-pinene+O_3 is much less than predicted by growth experiments.

4 Conclusions

Experimental observations of T-dependent SOA evaporation have been presented that demonstrate that the apparent volatility of α-pinene + O_3 SOA, as characterized by heating in a thermodenuder, is mostly independent of the SOA concentration over many orders of magnitude variation. Comparison of these observations with various kinetic models of evaporation in the TD suggest the observations are most consistent with SOA from the ozonolysis of α-pinene being composed of a large fraction of effectively non-volatile, but thermally-unstable species; these species are likely dimers or higher order oligomers, but could also be exceptionally low-volatility monomers. Any monomers that do exist must be of sufficiently low volatility (< ~1 μg m^{-3}) that they do not readily evaporate at room temperature. A dimer-decomposition model provided a good fit to the experimental observations when the monomer/dimer equilibrium constant ranged from K_{eqm} ~ 10^{-18} to 10^{-14} cm^3 $molecule^{-1}$, with corresponding rate coefficients for the reverse (decomposition) reaction ranging from $k_r(298K) = 1.6x10^{-3}$ to 2.8×10^{-2} s^{-1}, and a difference in activation energies between the forward and reverse rate coefficients ranging from ΔE_a = 15 to 42 kJ mol^{-1}. The best-fit dimer-decomposition model can also explain observations of slow rates of evaporation after isothermal dilution (Vaden et al., 2011;Wilson et al., 2015) and nearly constant composition as a function of rapid heating (Cappa and Wilson, 2011). These parameters would, by themselves, suggest that the SOA particles are nearly entirely composed of dimers, which seems unlikely. A model where the particle was assumed to be composed of low-volatility compounds — either highly oxygenated monomers or oligomers — could explain the bulk evaporation observations nearly as well, although suggested that large changes to particle composition upon heating should be observed. Thus, it seems that a hybrid model where the particles are composed of a substantial fraction of dimers (or oligomers) and some smaller fraction of low-volatility compounds may ultimately provide a more complete description.

Many laboratory (Cappa and Wilson, 2011;Emanuelsson et al., 2013;Loza et al., 2013;Grieshop et al., 2007;Saleh et al., 2013) and field studies (Cappa and Jimenez, 2010) have aimed to characterize the volatility of SOA. In general, the observations have concluded that the effective volatility of SOA is much lower than the volatility determined from interpretation of formation studies within a gas/particle partitioning framework. The analysis presented here suggests that this apparent discrepancy can be reconciled to a large extent through a combined

framework in which the volatility distributions derived from growth experiments (i.e. (Pathak et al., 2007)) provides a reasonable description of the properties of the condensing monomers, but where rapid formation of thermally-unstable dimers (and higher order oligomers) occurs, which consequently suppresses the apparent volatility of the SOA. Since the residence time in our flowtube was ~ 1 minute, these accretion reactions must occur on a similar timescale (or faster). This dimer formation timescale is much faster than what is typically used within air quality models (Carlton et al., 2010), which assume timescales on the order of a day, and suggests that air quality models may therefore have SOA that is too volatile and thus overly sensitive to dilution. However, care must be taken in the implementation of any model that allows for such rapid formation of dimers, as the ultimate consequence would be to transfer all semi-volatile material to the condensed phase. One possible reconciliation is that SOA particles may actually have a very high viscosity (which is, perhaps, a consequence of oligomer formation), which can limit the transport of gas-phase material into the particle bulk and the timescale and extent of transfer of gas-phase material into the particles (Zaveri et al., 2014). Although the oligomeric content of ambient biogenic SOA may be less than in laboratory biogenic SOA (Kourtchev et al., 2014) the presence of oligomers has been observed in both and needs to be accounted for in models of SOA volatility.

Author Contribution

K.R. Kolesar and C.D. Cappa designed the experiments and D. Johnson carried them out. C. Chen characterized the temperature profile in the thermodenuder. C.D. Cappa and K.R. Kolesar modified the kinetic model of evaporation from Cappa (2010) and performed the simulations. K.R. Kolesar and C.D. Cappa prepared the manuscript.

Acknowledgements

Special thanks to Anthony Kong for his assistance in running laboratory experiments. Funding for this work was provided by the National Science Foundation (ATM-1151062). K.R.K. was partially supported by a fellowship from the UC Davis Atmospheric Aerosols and Health program.

References

Abramson, E., Imre, D., Beranek, J., Wilson, J., and Zelenyuk, A.: Experimental determination of chemical diffusion within secondary organic aerosol particles, Physical Chemistry Chemical Physics, 15, 2983-2991, 10.1039/c2cp44013j, 2013.

Andreae, M. O., and Crutzen, P. J.: Atmospheric aerosols: Biogeochemical sources and role in atmospheric chemistry, Science, 276, 1052-1058, 10.1126/science.276.5315.1052, 1997.

Cappa, C. D.: A model of aerosol evaporation kinetics in a thermodenuder, Atmospheric Measurement Techniques, 3, 579-592, 10.5194/amt-3-579-2010, 2010.

Cappa, C. D., and Jimenez, J. L.: Quantitative estimates of the volatility of ambient organic aerosol, Atmospheric Chemistry and Physics, 10, 5409-5424, 10.5194/acp-10-5409-2010, 2010.

Cappa, C. D., and Wilson, K. R.: Evolution of organic aerosol mass spectra upon heating: implications for OA phase and partitioning behavior, Atmospheric Chemistry and Physics, 11, 1895-1911, 10.5194/acp-11-1895-2011, 2011.

Carlton, A. G., Bhave, P. V., Napelenok, S. L., Edney, E. D., Sarwar, G., Pinder, R. W., Pouliot, G. A., and Houyoux, M.: Model Representation of Secondary Organic Aerosol in CMAQv4.7, Environmental Science & Technology, 44, 8553-8560, 10.1021/es100636q, 2010.

Chen, Y. Y., Ebenstein, A., Greenstone, M., and Li, H. B.: Evidence on the impact of sustained exposure to air pollution on life expectancy from China's Huai River policy, Proceedings of the National Academy of Sciences of the United States of America, 110, 12936-12941, 10.1073/pnas.1300018110, 2013.

Donahue, N. M., Robinson, A. L., Stanier, C. O., and Pandis, S. N.: Coupled partitioning, dilution, and chemical aging of semivolatile organics, Environmental Science & Technology, 40, 02635-02643, 10.1021/es052297c, 2006.

Ehn, M., Thornton, J. A., Kleist, E., Sipila, M., Junninen, H., Pullinen, I., Springer, M., Rubach, F., Tillmann, R., Lee, B., Lopez-Hilfiker, F., Andres, S., Acir, I.-H., Rissanen, M., Jokinen, T., Schobesberger, S., Kangasluoma, J., Kontkanen, J., Nieminen, T., Kurten, T., Nielsen, L. B., Jorgensen, S., Kjaergaard, H. G., Canagaratna, M., Maso, M. D., Berndt, T., Petaja, T., Wahner, A., Kerminen, V.-M., Kulmala, M., Worsnop, D. R., Wildt, J., and Mentel, T. F.: A large source of low-volatility secondary organic aerosol, Nature, 506, 476-479, 10.1038/nature13032, 2014.

Emanuelsson, E. U., Watne, A. K., Lutz, A., Ljungstrom, E., and Hallquist, M.: Influence of Humidity, Temperature, and Radicals on the Formation and Thermal Properties of Secondary Organic Aerosol (SOA) from Ozonolysis of beta-Pinene, J. Phys. Chem. A, 117, 10346-10358, 10.1021/jp4010218, 2013.

Epstein, S. A., Riipinen, I., and Donahue, N. M.: A Semiempirical Correlation between Enthalpy of Vaporization and Saturation Concentration for Organic Aerosol, Environmental Science & Technology, 44, 743-748, 10.1021/es902497z, 2010.

Fuentes, E., and McFiggans, G.: A modeling approach to evaluate the uncertainty in estimating the evaporation behaviour and volatility of organic aerosols, Atmospheric Measurement Techniques, 5, 735-757, 10.5194/amt-5-735-2012, 2012.

Gao, S., Keywood, M., Ng, N. L., Surratt, J., Varutbangkul, V., Bahreini, R., Flagan, R. C., and Seinfeld, J. H.: Low-molecular-weight and oligomeric components in secondary organic aerosol

from the ozonolysis of cycloalkenes and alpha-pinene, J. Phys. Chem. A, 108, 10147-10164, 10.1021/jp047466e, 2004a.
Gao, S., Ng, N. L., Keywood, M., Varutbangkul, V., Bahreini, R., Nenes, A., He, J. W., Yoo, K. Y., Beauchamp, J. L., Hodyss, R. P., Flagan, R. C., and Seinfeld, J. H.: Particle phase acidity and oligomer formation in secondary organic aerosol, Environmental Science & Technology, 38, 6582-6589, 10.1021/es049125k, 2004b.
Grieshop, A. P., Donahue, N. M., and Robinson, A. L.: Is the gas-particle partitioning in alpha-pinene secondary organic aerosol reversible?, Geophysical Research Letters, 34, L14810 10.1029/2007gl029987, 2007.
Guenther, A., Hewitt, C. N., Erickson, D., Fall, R., Geron, C., Graedel, T., Harley, P., Klinger, L., Lerdau, M., McKay, W. A., Pierce, T., Scholes, B., Steinbrecher, R., Tallamraju, R., Taylor, J., and Zimmerman, P.: A Global-Model of Natural Volatile Organic-Compound Emissions, J. Geophys. Res.-Atmos., 100, 8873-8892, 10.1029/94jd02950, 1995.
Hall, W. A., and Johnston, M. V.: Oligomer Formation Pathways in Secondary Organic Aerosol from MS and MS/MS Measurements with High Mass Accuracy and Resolving Power, J. Am. Soc. Mass Spectrom., 23, 1097-1108, 10.1007/s13361-012-0362-6, 2012a.
Hall, W. A., and Johnston, M. V.: The Thermal-Stability of Oligomers in Alpha-Pinene Secondary Organic Aerosol, Aerosol Science and Technology, 46, 983-989, 10.1080/02786826.2012.685114, 2012b.
Hallquist, M., Wenger, J. C., Baltensperger, U., Rudich, Y., Simpson, D., Claeys, M., Dommen, J., Donahue, N. M., George, C., Goldstein, A. H., Hamilton, J. F., Herrmann, H., Hoffmann, T., Iinuma, Y., Jang, M., Jenkin, M. E., Jimenez, J. L., Kiendler-Scharr, A., Maenhaut, W., McFiggans, G., Mentel, T. F., Monod, A., Prevot, A. S. H., Seinfeld, J. H., Surratt, J. D., Szmigielski, R., and Wildt, J.: The formation, properties and impact of secondary organic aerosol: current and emerging issues, Atmospheric Chemistry and Physics, 9, 5155-5236, 2009.
Han, Y. M., Iwamoto, Y., Nakayama, T., Kawamura, K., and Mochida, M.: Formation and evolution of biogenic secondary organic aerosol over a forest site in Japan, J. Geophys. Res.-Atmos., 119, 259-273, 10.1002/2013jd020390, 2014.
Henry, K. M., Lohaus, T., and Donahue, N. M.: Organic Aerosol Yields from alpha-Pinene Oxidation: Bridging the Gap between First-Generation Yields and Aging Chemistry, Environmental Science & Technology, 46, 12347-12354, 10.1021/es302060y, 2012.
Huffman, J. A., Ziemann, P. J., Jayne, J. T., Worsnop, D. R., and Jimenez, J. L.: Development and characterization of a fast-stepping/scanning thermodenuder for chemically-resolved aerosol volatility measurements, Aerosol Science and Technology, 42, 395-407, 10.1080/02786820802104981, 2008.
Kalberer, M., Paulsen, D., Sax, M., Steinbacher, M., Dommen, J., Prevot, A. S. H., Fisseha, R., Weingartner, E., Frankevich, V., Zenobi, R., and Baltensperger, U.: Identification of polymers as major components of atmospheric organic aerosols, Science, 303, 1659-1662, 10.1126/science.1092185, 2004.
Kannosto, J., Yli-Pirila, P., Hao, L. Q., Leskinen, J., Jokiniemi, J., Makela, J. M., Joutsensaari, J., Laaksonen, A., Worsnop, D. R., Keskinen, J., and Virtanen, A.: Bounce characteristics of alpha-pinene-derived SOA particles with implications to physical phase, Boreal Environment Research, 18, 329-340, 2013.
Karnezi, E., Riipinen, I., and Pandis, S. N.: Measuring the atmospheric organic aerosol volatility distribution: a theoretical analysis, Atmos. Meas. Tech., 2953–2965, 10.5194/amt-7-2953-2014, 2014.

Kesselmeier, J., and Staudt, M.: Biogenic volatile organic compounds (VOC): An overview on emission, physiology and ecology, Journal of Atmospheric Chemistry, 33, 23-88, 10.1023/a:1006127516791, 1999.

Koop, T., Bookhold, J., Shiraiwa, M., and Poschl, U.: Glass transition and phase state of organic compounds: Dependency on molecular properties and implications for secondary organic aerosols in the atmosphere, Physical Chemistry Chemical Physics, 13, 19238-19255, 10.1039/c1cp22617g, 2011.

Kostenidou, E., Lee, B. H., Engelhart, G. J., Pierce, J. R., and Pandis, S. N.: Mass Spectra Deconvolution of Low, Medium, and High Volatility Biogenic Secondary Organic Aerosol, Environmental Science & Technology, 43, 4884-4889, 10.1021/es803676g, 2009.

Kourtchev, I., Fuller, S. J., Giorio, C., Healy, R. M., Wilson, E., O'Connor, I., Wenger, J. C., McLeod, M., Aalto, J., Ruuskanen, T. M., Maenhaut, W., Jones, R., Venables, D. S., Sodeau, J. R., Kulmala, M., and Kalberer, M.: Molecular composition of biogenic secondary organic aerosols using ultrahigh-resolution mass spectrometry: comparing laboratory and field studies, Atmospheric Chemistry and Physics, 14, 2155-2167, 10.5194/acp-14-2155-2014, 2014.

Kristensen, K., Enggrob, K. L., King, S. M., Worton, D. R., Platt, S. M., Mortensen, R., Rosenoern, T., Surratt, J. D., Bilde, M., Goldstein, A. H., and Glasius, M.: Formation and occurrence of dimer esters of pinene oxidation products in atmospheric aerosols, Atmos. Chem. Phys., 13, 3763-3776, 10.5194/acp-13-3763-2013, 2013.

Kristensen, K., Cui, T., Zhang, H., Gold, A., Glasius, M., and Surratt, J. D.: Dimers in alpha-pinene secondary organic aerosol: effect of hydroxyl radical, ozone, relative humidity and aerosol acidity, Atmospheric Chemistry and Physics, 14, 4201-4218, 10.5194/acp-14-4201-2014, 2014.

Kundu, S., Fisseha, R., Putman, A. L., Rahn, T. A., and Mazzoleni, L. R.: High molecular weight SOA formation during limonene ozonolysis: insights from ultrahigh-resolution FT-ICR mass spectrometry characterization, Atmospheric Chemistry and Physics, 12, 5523-5536, 10.5194/acp-12-5523-2012, 2012.

Lee, B. H., Kostenidou, E., Hildebrandt, L., Riipinen, I., Engelhart, G. J., Mohr, C., DeCarlo, P. F., Mihalopoulos, N., Prevot, A. S. H., Baltensperger, U., and Pandis, S. N.: Measurement of the ambient organic aerosol volatility distribution: application during the Finokalia Aerosol Measurement Experiment (FAME-2008), Atmospheric Chemistry and Physics, 10, 12149-12160, 10.5194/acp-10-12149-2010, 2010.

Lee, B. H., Pierce, J. R., Engelhart, G. J., and Pandis, S. N.: Volatility of secondary organic aerosol from the ozonolysis of monoterpenes, Atmos. Environ., 45, 2443-2452, 10.1016/j.atmosenv.2011.02.004, 2011.

Loza, C. L., Coggon, M. M., Nguyen, T. B., Zuend, A., Flagan, R. C., and Seinfeld, J. H.: On the Mixing and Evaporation of Secondary Organic Aerosol Components, Environmental Science & Technology, 47, 6173-6180, 10.1021/es400979k, 2013.

Matsunaga, A., and Ziemann, P. J.: Yields of beta-hydroxynitrates, dihydroxynitrates, and trihydroxynitrates formed from OH radical-initiated reactions of 2-methyl-1-alkenes, Proceedings of the National Academy of Sciences of the United States of America, 107, 6664-6669, 10.1073/pnas.0910585107, 2010.

Muller, L., Reinnig, M. C., Hayen, H., and Hoffmann, T.: Characterization of oligomeric compounds in secondary organic aerosol using liquid chromatography coupled to electrospray ionization Fourier transform ion cyclotron resonance mass spectrometry, Rapid Communications in Mass Spectrometry, 23, 971-979, 10.1002/rcm.3957, 2009.

Odum, J. R., Hoffmann, T., Bowman, F., Collins, D., Flagan, R. C., and Seinfeld, J. H.: Gas/particle partitioning and secondary organic aerosol yields, Environmental Science & Technology, 30, 2580-2585, 1996.
Pankow, J. F.: An Absorption-Model of the Gas Aerosol Partitioning Involved in the Formation of Secondary Organic Aerosol, Atmos. Environ., 28, 189-193, 1994.
Pathak, R. K., Presto, A. A., Lane, T. E., Stanier, C. O., Donahue, N. M., and Pandis, S. N.: Ozonolysis of alpha-pinene: parameterization of secondary organic aerosol mass fraction, Atmospheric Chemistry and Physics, 7, 3811-3821, 2007.
Putman, A. L., Offenberg, J. H., Fisseha, R., Kundu, S., Rahn, T. A., and Mazzoleni, L. R.: Ultrahigh-resolution FT-ICR mass spectrometry characterization of alpha-pinene ozonolysis SOA, Atmos. Environ., 46, 164-172, 10.1016/j.atmosenv.2011.10.003, 2012.
Riipinen, I., Pierce, J. R., Donahue, N. M., and Pandis, S. N.: Equilibration time scales of organic aerosol inside thermodenuders: Evaporation kinetics versus thermodynamics, Atmos. Environ., 44, 597-607, 10.1016/j.atmosenv.2009.11.022, 2010.
Roldin, P., Eriksson, A. C., Nordin, E. Z., Hermansson, E., Mogensen, D., Rusanen, A., Boy, M., Swietlicki, E., Svenningsson, B., Zelenyuk, A., and Pagels, J.: Modelling non-equilibrium secondary organic aerosol formation and evaporation with the aerosol dynamics, gas- and particle-phase chemistry kinetic multilayer model ADCHAM, Atmospheric Chemistry and Physics, 14, 7953-7993, 10.5194/acp-14-7953-2014, 2014.
Saleh, R., Shihadeh, A., and Khlystov, A.: On transport phenomena and equilibration time scales in thermodenuders, Atmospheric Measurement Techniques, 4, 571-581, 10.5194/amt-4-571-2011, 2011.
Saleh, R., Donahue, N. M., and Robinson, A. L.: Time Scales for Gas-Particle Partitioning Equilibration of Secondary Organic Aerosol Formed from Alpha-Pinene Ozonolysis, Environmental Science & Technology, 47, 5588-5594, 10.1021/es400078d, 2013.
Salo, K., Hallquist, M., Jonsson, A. M., Saathoff, H., Naumann, K. H., Spindler, C., Tillmann, R., Fuchs, H., Bohn, B., Rubach, F., Mentel, T. F., Muller, L., Reinnig, M., Hoffmann, T., and Donahue, N. M.: Volatility of secondary organic aerosol during OH radical induced ageing, Atmospheric Chemistry and Physics, 11, 11055-11067, 10.5194/acp-11-11055-2011, 2011.
Saxena, P., and Hildemann, L. M.: Water-soluble organics in atmospheric particles: A critical review of the literature and application of thermodynamics to identify candidate compounds, Journal of Atmospheric Chemistry, 24, 57-109, 1996.
Seinfeld, J. H., and Pankow, J. F.: Organic atmospheric particulate material, Annu. Rev. Phys. Chem., 54, 121-140, 10.1146/annurev.physchem.54.011002.103756, 2003.
Shilling, J. E., Chen, Q., King, S. M., Rosenoern, T., Kroll, J. H., Worsnop, D. R., DeCarlo, P. F., Aiken, A. C., Sueper, D., Jimenez, J. L., and Martin, S. T.: Loading-dependent elemental composition of alpha-pinene SOA particles, Atmospheric Chemistry and Physics, 9, 771-782, 2009.
Stanier, C. O., Pathak, R. K., and Pandis, S. N.: Measurements of the volatility of aerosols from alpha-piniene ozonolysis, Environmental Science & Technology, 41, 2756-2763, 10.1021/es0519280, 2007.
Tolocka, M. P., Jang, M., Ginter, J. M., Cox, F. J., Kamens, R. M., and Johnston, M. V.: Formation of oligomers in secondary organic aerosol, Environmental Science & Technology, 38, 1428-1434, 10.1021/es035030r, 2004.

Trump, E. R., and Donahue, N. M.: Oligomer formation within secondary organic aerosols: equilibrium and dynamic considerations, Atmospheric Chemistry and Physics, 14, 3691-3701, 10.5194/acp-14-3691-2014, 2014.
Vaden, T. D., Imre, D., Beránek, J., Shrivastava, M., and Zelenyuk, A.: Evaporation kinetics and phase of laboratory and ambient secondary organic aerosol, Proceedings of the National Academy of Sciences of the United States of America, 108, 2190-2195, 10.1073/pnas.1013391108, 2011.
Virtanen, A., Joutsensaari, J., Koop, T., Kannosto, J., Yli-Pirila, P., Leskinen, J., Makela, J. M., Holopainen, J. K., Poschl, U., Kulmala, M., Worsnop, D. R., and Laaksonen, A.: An amorphous solid state of biogenic secondary organic aerosol particles, Nature, 467, 824-827, 10.1038/nature09455, 2010.
Weber, R. J., Sullivan, A. P., Peltier, R. E., Russell, A., Yan, B., Zheng, M., de Gouw, J., Warneke, C., Brock, C., Holloway, J. S., Atlas, E. L., and Edgerton, E.: A study of secondary organic aerosol formation in the anthropogenic-influenced southeastern United States, J. Geophys. Res.-Atmos., 112, 10.1029/2007jd008408, 2007.
Wilson, J., Imre, D., Beranek, J., Shrivastava, M., and Zelenyuk, A.: Evaporation Kinetics of Laboratory-Generated Secondary Organic Aerosols at Elevated Relative Humidity, Environmental Science & Technology, 49, 243-249, 2015.
Yasmeen, F., Vermeylen, R., Szmigielski, R., Iinuma, Y., Boge, O., Herrmann, H., Maenhaut, W., and Claeys, M.: Terpenylic acid and related compounds: precursors for dimers in secondary organic aerosol from the ozonolysis of alpha- and beta-pinene, Atmospheric Chemistry and Physics, 10, 9383-9392, 10.5194/acp-10-9383-2010, 2010.
Zaveri, R. A., Easter, R. C., Shilling, J. E., and Seinfeld, J. H.: Modeling kinetic partitioning of secondary organic aerosol and size distribution dynamics: representing effects of volatility, phase state, and particle-phase reaction, Atmospheric Chemistry and Physics, 14, 5153-5181, 10.5194/acp-14-5153-2014, 2014.
Zhang, Q., Worsnop, D. R., Canagaratna, M. R., and Jimenez, J. L.: Hydrocarbon-like and oxygenated organic aerosols in Pittsburgh: insights into sources and processes of organic aerosols, Atmospheric Chemistry and Physics, 5, 3289-3311, 2005.
Zhang, X., Cappa, C. D., Jathar, S. H., McVay, R. C., Ensberg, J. J., Kleeman, M. J., and Seinfeld, J. H.: Influence of vapor wall loss in laboratory chambers on yields of secondary organic aerosol, Proceedings of the National Academy of Sciences of the United States of America, 111, 5802-5807, 10.1073/pnas.1404727111, 2014.

Table 1. Experimental conditions for α-pinene + O_3 SOA generation for the various experiments.

Experiment Date	Flowrate (lpm)	Initial C_{OA} (μg m^{-3})	C_{OA} after dilution (μg m^{-3})	α-pinene (μL hr^{-1})	Ozone (ppm)	$d_{p,V,bypass}$ (nm)
90512	0.79	1	n/a	0.12	4.9	37
82912	0.8	9	n/a	0.12	7.8	39
101912	0.8	30	n/a	0.6	8.8	52
41114	0.82	90	n/a	0.15	38.7	48
90712	0.81	150	n/a	0.3	6.8	61
91312	0.8	180	n/a	0.2	^	57
40914	0.82	200	n/a	0.23*	63	57
91212	0.8	400	n/a	0.5	^	73
101612	0.8	450	n/a	0.6	8.8	83
101712	0.8	500	n/a	0.6	8.8	88
91112	0.8	600	n/a	0.38	23.4	76
101812	0.83	800	n/a	0.6	8.8	97
101212	0.83	380	5	0.6	8.8	73
100912	1.02	380	6	0.7	9.8	71
101112	0.79	430	7	0.5	9.7	73
101012	0.8	450	10	0.5	8.8	77
83112	0.8	600	14	0.5	29.3	76
92412	0.76	650	23	0.5	9.7	90
100412	1.04	450	23	0.5	8.8	68

* The flowrate of N_2 over the α-pinene syringe was 0.015 lpm for all experiments except this one, for which it was 0.074 lpm.
^ Unknown

Table 2. The average fit parameters for each C_{OA} grouping of mass thermograms.

Mass Loading Range ($\mu g\ m^{-3}$)	$S_{VFR} \pm \sigma_e$ [#]	$T_{50} \pm \sigma_e$ (K)	# of Samples
Diluted (<23)	-15.9 ± 1.6	346 ± 7	7
Low (≤30)	-16.6 ± 1.9	345 ± 5	3
Medium ($90 < C_{OA} < 200$)	-15.7 ± 1.6	347 ± 6	4
High (>300)	-16.4 ± 1.5	359 ± 7	5

[#] σ_e is the greater of the propagation of error from the individual fits and the sample standard deviation.

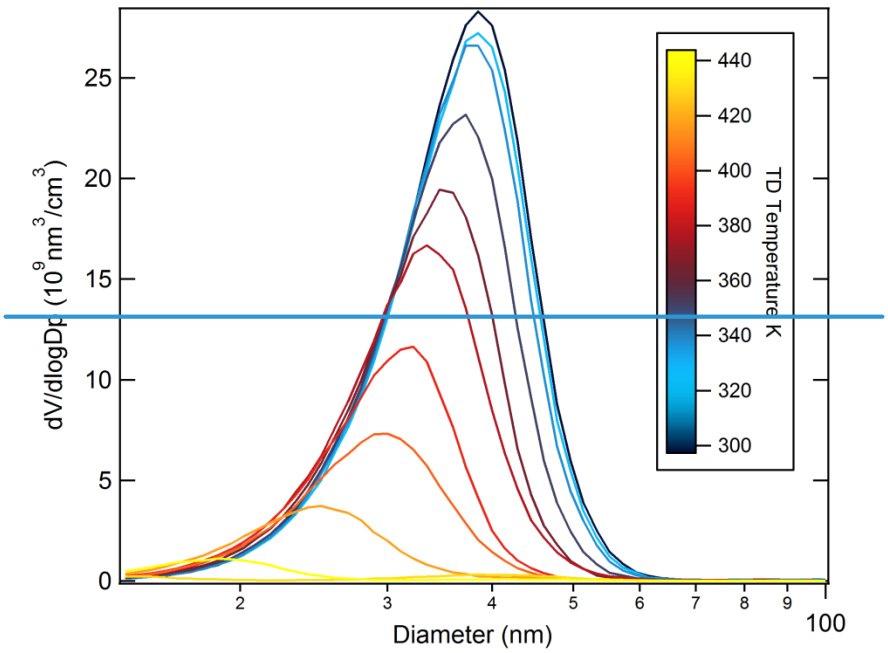

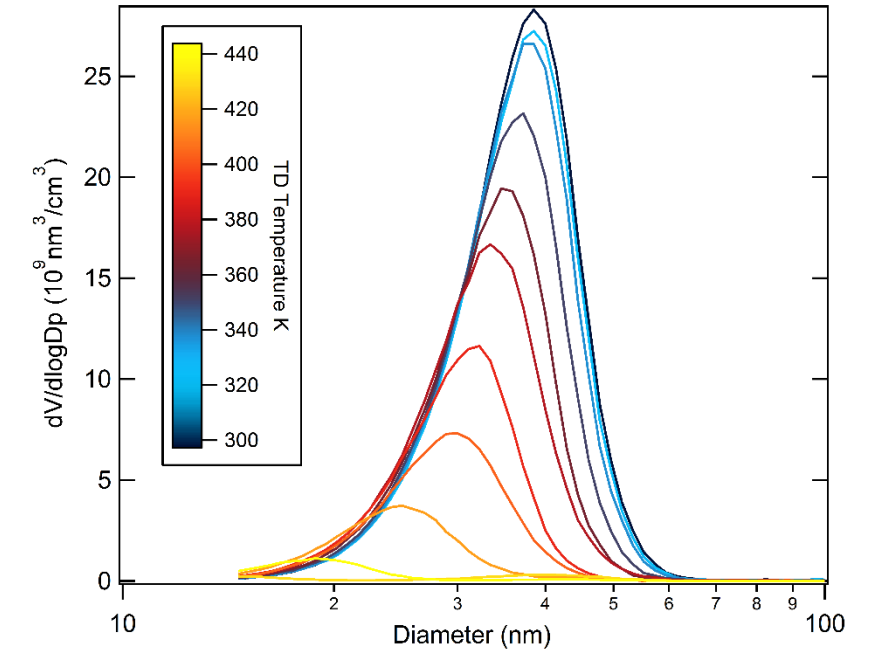

Figure 1. An example of the particle volume weighted size distributions observed as a function of TD temperature from one experiment. The temperatures range from room temperature (296 K, light blue) to 453 K (purple). This experiment had a bypass C_{OA} = 9µg m^{-3} and $d_{p,V,bypass}$ = 39 nm.

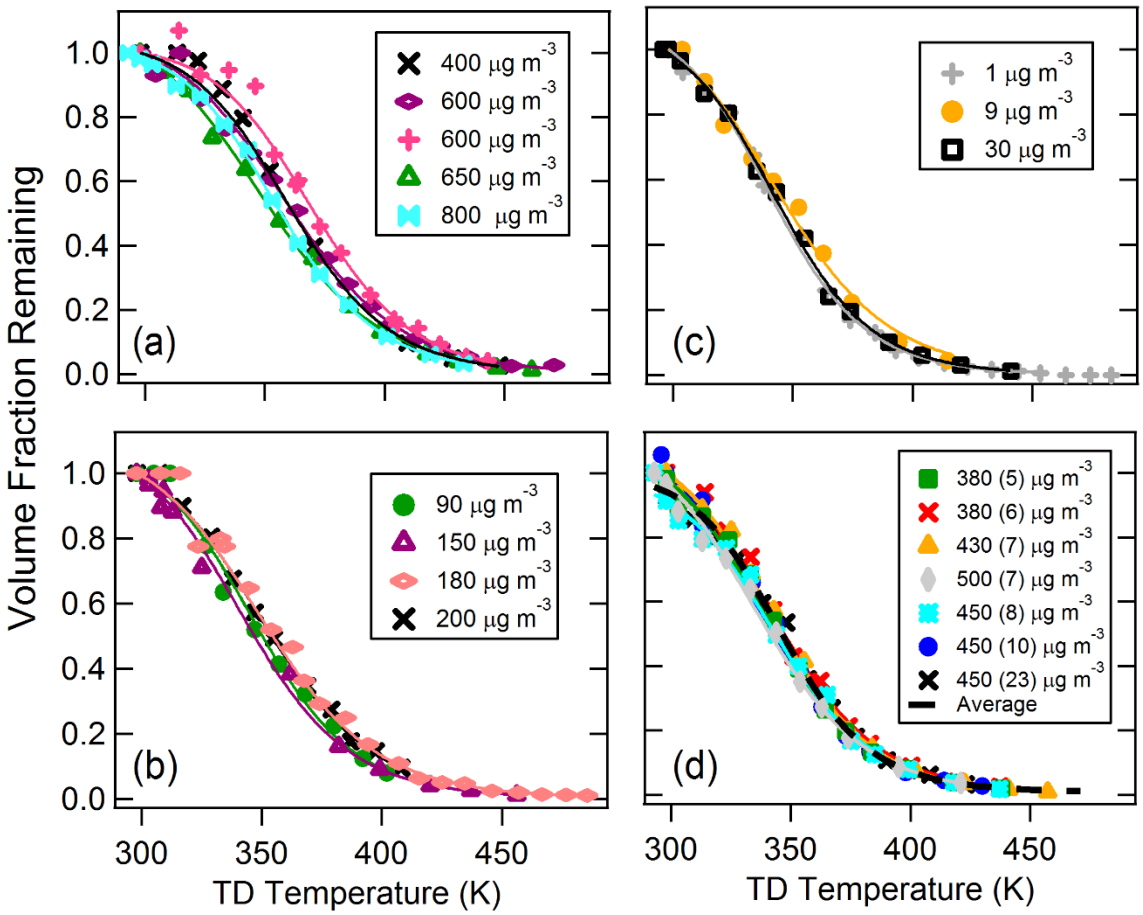

Figure 2. Mass thermograms measured for each of the experiments (symbols). Results are grouped according to the bypass mass loading as (a) high ($C_{OA} > 300$ μg m^{-3}), (b) medium ($90 \leq C_{OA} < 300$ μg m^{-3}), and (c) low loading ($C_{OA} \leq 30$ μg m^{-3}). Results from isothermal dilution experiments are shown in (d), where the initial number is the C_{OA} before dilution and the number in parentheses that after dilution. Traces represent the fit of Eq. 2 to each experiment.

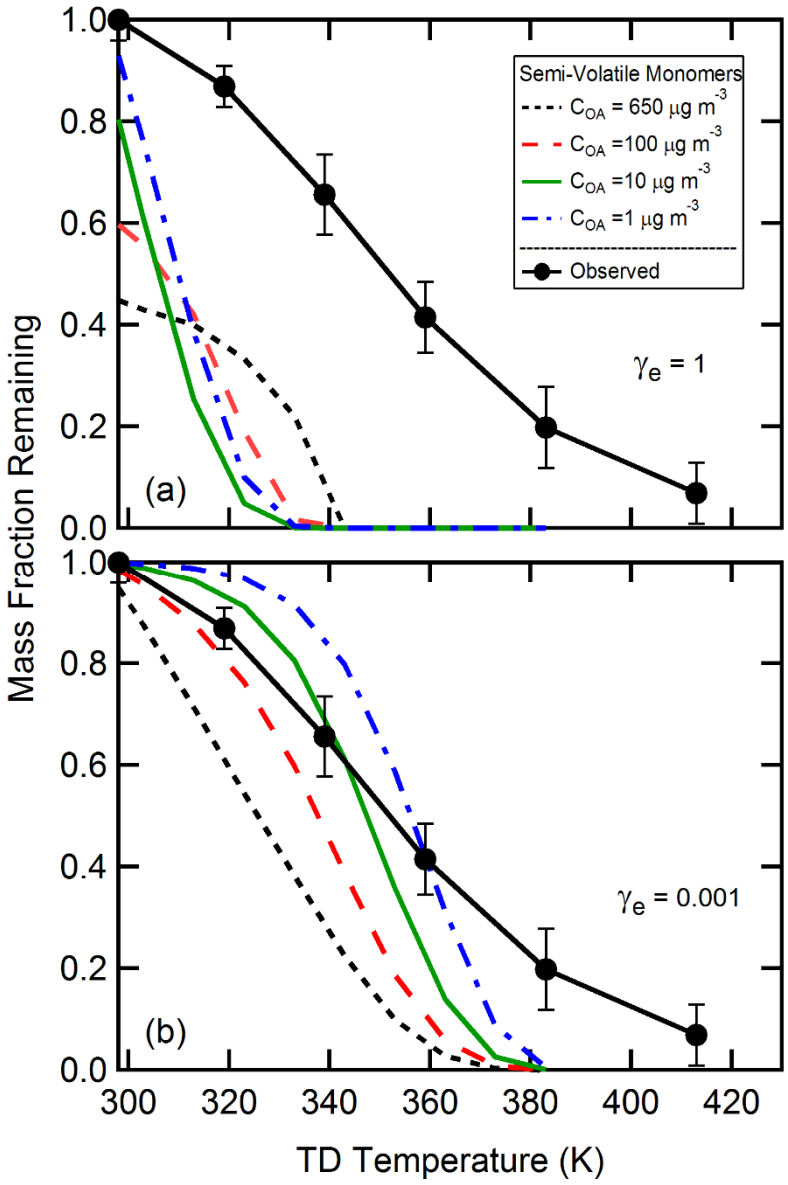

Figure 3. Model predictions for the mass thermograms of α-pinene+O_3 SOA using the semi-volatile monomer TD model where the initial model C_{OA} was 650 μg m^{-3} (black, short dash), 100 μg m^{-3} (red, long dash), 10 μg m^{-3} (green, solid) or 1 μg m^{-3} (blue, dot-dash) for evaporation coefficients, γ_e, equal to (a) 1 and (b) 0.001. Neither set of predictions agree well with the observed mass thermogram for medium/low C_{OA} (black line with black ●).

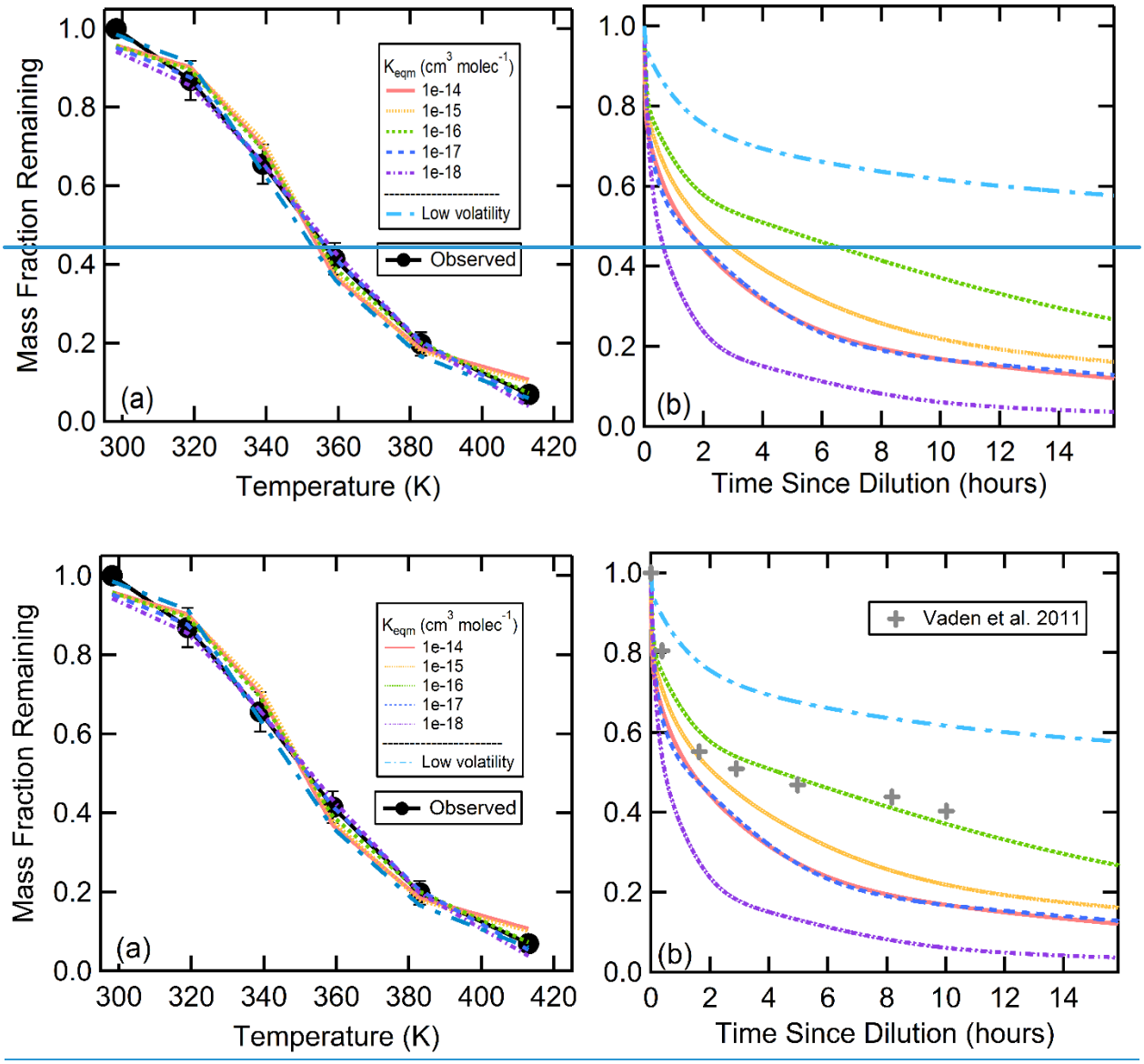

Figure 4. (a) Comparison between observed medium/low C_{OA} grouping (black ●) and best-fit calculated mass thermograms for the TD model that includes dimer decomposition and for the low-volatility compound model. For the dimer-decomposition model, the concentration of dimers is much greater than the concentration of monomers. (b) Simulated isothermal, room temperature evaporation based on the best-fit model parameters determined in (a). The initial SOA concentration was 100 µg m^{-3}, which was diluted by a factor of 30 and evaporated vapors were lost to the simulated chamber walls with a rate coefficient of 10^{-3} s^{-1}. The grey crosses (+) in panel b are the experimental data from the isothermal dilution of α-pinene+O_3 SOA (d_p = 160 nm) from Vaden et al. (2011).

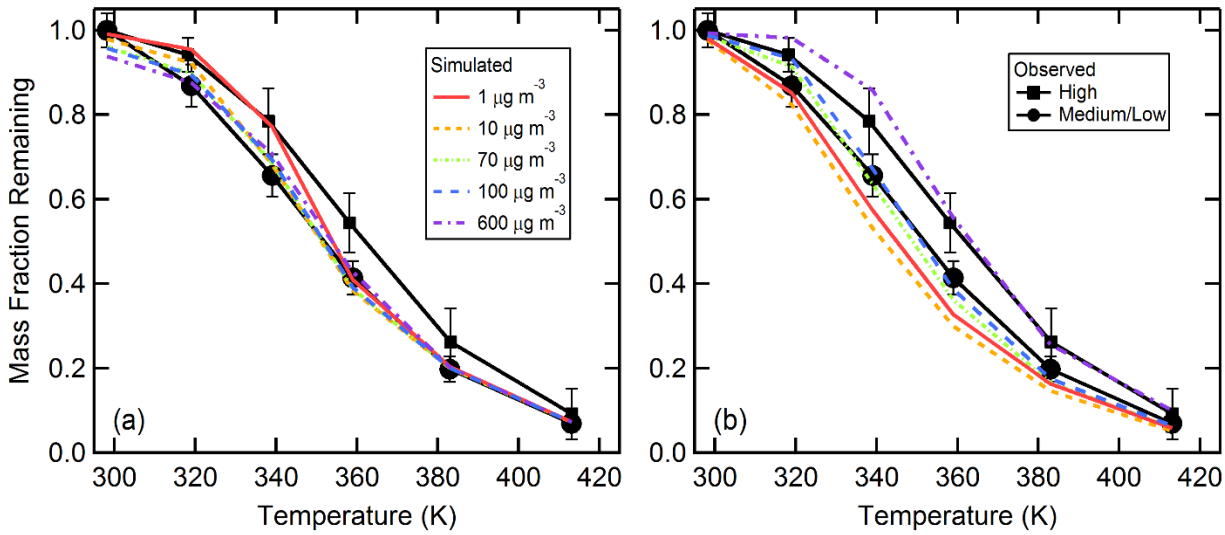

Figure 5. (a) Calculated mass thermograms for variable C_{OA} based on the best-fit parameters for the $K_{eqm} = 10^{-16}$ cm^3 molecules^{-1} dimer-decomposition model as compared to the observations for the average medium/low and high C_{OA}. (b) Same as (a), but for the best-fit low-volatility model.

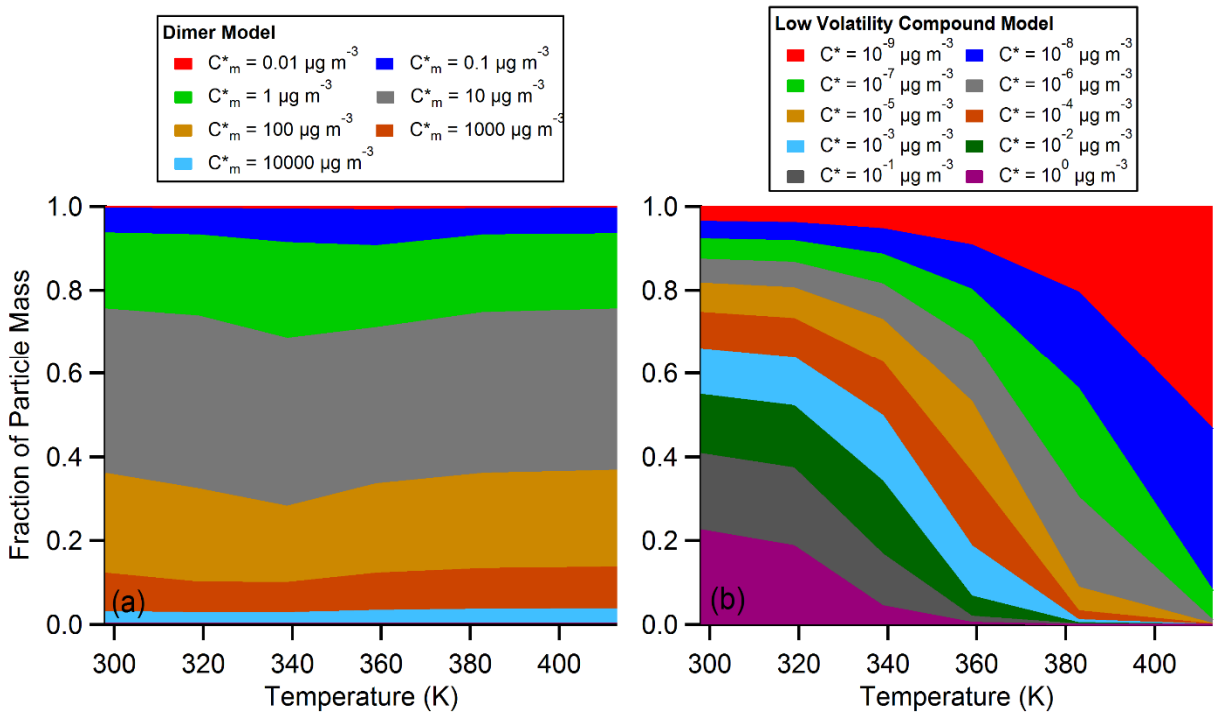

Figure 6. Variation in the relative particle composition with temperature from the (a) dimer-decomposition and (b) low-volatility monomer evaporation TD models. The colors correspond to the various dimer and monomer species, defined by the monomer C^* values. For the dimer-decomposition model the monomer fractional contributions are too small to be seen, and the reported C^* values in the legend correspond to the parent monomer values associated with each dimer. For the low-volatility monomer case, the C^* values correspond to the actual evaporating monomer values. The simulations were run for an initial C_{OA} = 100 µg m^{-3}.

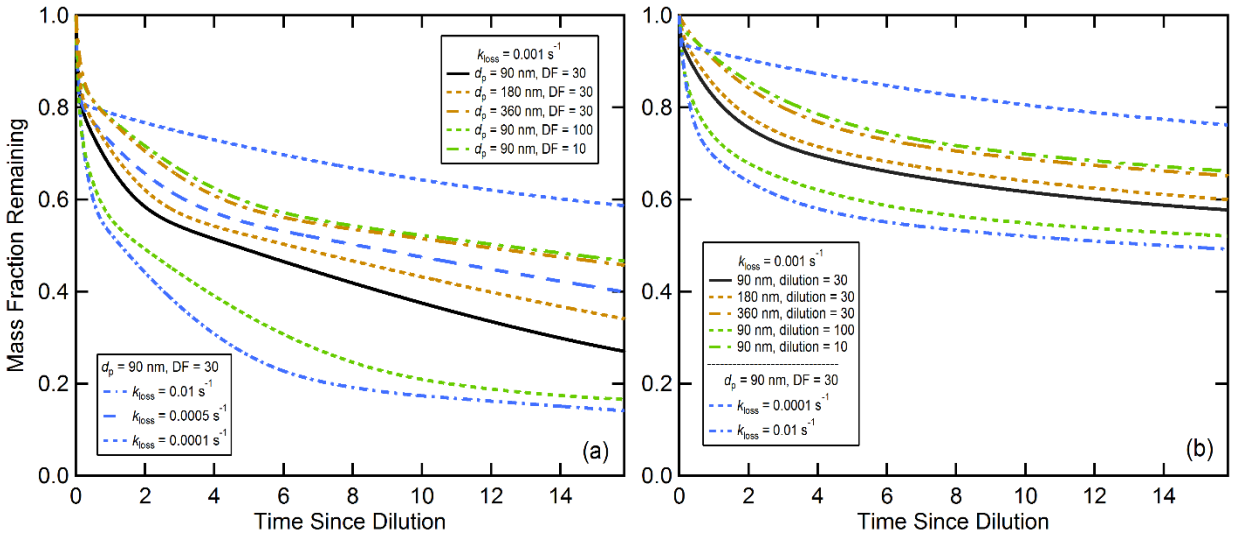

Figure 7. Dependence of the isothermal evaporation simulations on the assumed vapor loss rate (k_{loss}), dilution factor (DF) or particle diameter (d_p) for (a) the dimer-decomposition and (b) the low-volatility models. All simulations were run for an initial C_{OA} = 100 µg m^{-3}. For the dimer-decomposition model, the K_{eqm} = 10^{-16} cm^3 molecules^{-1} best-fit results were used.